Spring 2018

New Method of Nickel Oxide as Hole Transport Layer and Characteristics of Nickel Oxide Based Perovskite Solar Cell

Loi Nguyen
Old Dominion University

NEW METHOD OF NICKEL OXIDE AS HOLE TRANSPORT LAYER AND CHARACTERISTICS OF NICKEL OXIDE BASED PEROVSKITE SOLAR CELL

by

Loi Nguyen
A.A. December 2015, University of Maryland University College
B.S. May 2017, Old Dominion University

A Thesis Submitted to the Faculty of
Old Dominion University in Partial Fulfillment of the
Requirements for the Degree of

MASTER OF SCIENCE

ELECTRICAL AND COMPUTER ENGINEERING

OLD DOMINION UIVERSITY
May 2018

Approved by:

Gon Namkoong (Director)

Helmut Baumgart (Member)

Hani Elsayed-Ali (Member)

ABSTRACT

NEW METHOD OF NICKEL OXIDE AS HOLE TRANSPORT LAYER AND CHARACTERISTICS OF NICKEL OXIDE BASED PEROVSKITE SOLAR CELL

Loi Nguyen
Old Dominion University, 2018
Director: Dr. Gon Namkoong

For perovskite solar cells, poly (2,3-dihydrothieno-1, 4-dioxin)-poly (styrenesulfonate) (PEDOT:PSS) is a common hole transport layer. However, PEDOT:PSS has a lot of drawbacks, such as irregular quality from distributors, poor electron blocker, and hygroscopic nature. On the other hand, NiO_x has been reported that it can provide good stability and carrier mobility. From literature, NiO_x was used to replace PEDOT:PSS as a hole transport layer with positive results since it is transparent as a thin film and also possesses compatible work function in perovskite solar cell bandgap alignment. In depositing NiO_x as a thin film, many approaches have been developed. However, those approaches required the use of acute toxic chemicals, lengthy processing time, complicated chemical requirement, and/ or expensive equipment. In order to obtain NiO_x thin film as a hole transport layer, we have developed a facile method to obtain a thin film of NiOx by simply mixing NiO_x powder and HCl solution. This process only needs less than 5 minutes of chemical mixing time and the precursor can be immediately spin-coated on top of substrate. In addition, the equipment needed to obtain thin film NiO_x is a spin coater and a hot plate.

With our quick, simple and inexpensive approach to get NiO_x thin film for perovskite solar cells with inverted p-i-n structure, it is found that inverted perovskite solar cell with NiO_x as a hole transport layer demonstrated higher open circuit voltage than perovskite solar cell fabricated with

PEDOT:PSS, which enhanced solar cell power conversion efficiency. Our experiment has shown that NiO_x thin film obtained by newly developed technique, exhibited promising material characteristics such as long lifetime decay. In our experiment, we also optimized the processing conditions of NiO_x thin films to remove the light soaking effect caused by defects in NiO_x layer. Hence, it is found that a quick, simple and inexpensive method enabled deposition of NiO_x thin film as a promising hole transport layer for inverted p-i-n structure of perovskite solar cell.

This thesis is dedicated to my mother, my brother, my sister, and my wife.

They believed in my dream for a college education in the U.S.

ACKNOWLEDGMENTS

I would like to thank Dr. Gon Namkoong in giving me the chance to become an undergraduate lab assistant since the beginning of my undergraduate program at Old Dominion University. It was a strong kick-start for me to learn how to perform research and to familiarize myself with different lab instruments. There were many interesting research projects and not all of them were easy. Dr. Namkoong has guided me through them all to eventually have my name recognized in one of his high impact published papers. Finally, Dr. Namkoong pushed me to this accomplishment.

I also would like to extend my appreciation to Dr. Hani Elsayed-Ali and Dr. Helmut Baumgart. They were so nice in becoming members of my thesis committee. The knowledge that they impacted me with made the finalization of this manuscript possible.

It was a long journey for me and I have met great people who were always willing to share their knowledge. Among all of the great people, Grace Rajan, Xin Chen and Pengtao Lin were always willing to spend their time to answer my spontaneous questions with a smile. The best teammates I could have ever asked for: Abdulla Al Mamun, Tanzila Tasnim Ava, Christine Gausin, and Jonny Blincoe. We spent so much time doing research together and all of you have taught me, guided me, helped me, and laughed at me so much. I loved it.

There have been days that I thought I could not have made it to this point. Besides family and research team, I would like to thank all members of FIRE lab for the encouragement and support: Michael O'Brien, Alfred Hammett, Dr. Rand Chandler, Julie Machamer, Aidan Cowhig, and Adam Daniels.

This work is supported by the NSF SoLEAP program.

TABLE OF CONTENTS

Page

LIST OF TABLES

Table Page

LIST OF FIGURES

Figure Page

Figure Page

CHAPTER I

INTRODUCTION

The finite amount of fossil fuel is pushing the world toward renewable source of energies. Solar energy is a popular renewable source of energy because of its easily accessible characteristics both on earth surface and outer space. Effort has been invested to increase the solar energy conversion efficiency as well as to lower the cost of solar energy harvesting devices. In the realm of photovoltaic field, there are many technologies being developed to transform solar energy to electrical energy such as organic solar cells [1]–[3], inorganic solar cells [4], [5], quantum dot solar cells [6], and dye-sensitized solar cells [7]–[13]. Solar power is the most reliable solution for a wide range of missions from low Earth surface all the way to Jupiter and outer space explorations. Therefore, solar cells are being used extensively for all type of aeronautics and space operations. However, with increasing mission demands, traditional solar cells such as the widely used silicon solar cells are proving to be inadequate in power efficiency, flexibility, and cost. Fortunately, there is a new solar cell technology called perovskite solar cell (PSC) in development which possesses promising capabilities such as low cost, flexibility, and potentially very high-power efficiency. Furthermore, perovskite solar cell technology has a lot of future potential since it has big absorption range [14], great extinction coefficient [15], [16], and long diffusion length [13], [17], [18]. Notably, a form of perovskite named methyl ammonium lead iodide ($CH_3NH_3PbX_3$) demonstrates excellent features such as big optical cross section [15], great charge transport [19], adjustable band gap [20]–[22], and this material is compatible with low-cost large-scale production technique [13]. Particularly, the PSC can be manufactured at low temperatures, but the efficiency can reach beyond 20% [23]. According to the NREL Efficiency Chart, the current perovskite solar

cell is at 22.1% efficiency, which is quite an improvement considering its founding efficiency to be 3.8% in 2009 [24]. Perovskite cells have the advantages in areas of being lightweight, flexible and have high efficiencies that provide low load when launching a spacecraft to space. These features are essential in enabling future NASA robotic and human exploration missions because perovskite solar technology not only increases the mission life, but also decreases mission mass. Being able to reach a high efficiency for PSCs means that we must understand the platform of its fabrication, the structure, as well as the issues relating to its anomalies and defects. The design of optimal device parameters is of paramount importance to achieve higher energy conversion efficiency in perovskite solar cells. For example, optical absorption and subsequent creation of photo-generated charge carriers, and extraction to electricity should be simultaneously optimized. In addition, the degradation of perovskite solar cells is one of the impending challenges to be overcome for commercialization of perovskite solar cells.

HISTORY OF PEROVSKITE SOLAR CELLS

With various properties such as ambipolar conductivity and good optical absorption that makes it a promising material, perovskite has been on the rise of research material in the solar market since it was found in 1839 by Gustav Rose [25]. Perovskite crystal structure was named after a Russian mineralogist Lev Perovskite [26], [27]. The perovskite crystal structure is identified with ABX_3 formation, of which A is a 2+ metal cation, B is a 4+ metal cation, and X is a 2- oxygen anion. $CaTiO_3$ and $BaTiO_3$ are popular perovskite structures [27]. In 1893, another ABX_3 composition was found by Wells [28]. In this new structure, A is a 1+ alkaline cation, B is a 2+ lead cation and X is a 1- halogen anion [27], [28]. In 1978, methyl ammonium cation ($CH_3NH_3^+$) was found to be able to replaced 1+ alkaline cation in perovskite structure [27], [29]. In 1995, this

organo-lead-halide perovskite structure $CH_3NH_3PbX_3$ was found to demonstrate semiconductor behaviors [27], [30]. The finding had a lot of impact in the research community and resulted in the Core Research for Evolutional Science and Technology (CREST) project in Japan. In 2009, the first dye-sensitized perovskite solar cells paper was published by Kojima et al. with the help of one of the CREST's researchers [24], [27]. However, because of the low efficiency and instability of this dye-sensitized perovskite solar cells structure, the research effort stopped [27]. In 2012, two different teams published perovskite solar cells with efficiency close to 10% [27], [31], [32]. The stunning achievement renewed the solar cell community's interest in perovskite structure. In the subsequence years, the efficiency of organo-lead-halide perovskite solar cells quickly reached 20% [27], [33]–[37]. In 2015, a certified efficiency of 22.6% was achieved by Jeon et al [27], [37]. Since the organo-lead-halide perovskite solar cells attained comparable efficiency with silicon solar cells, perovskite solar cells' structure and fabrication technique needed to be optimized for commercial viability. Factors such as stability, cost, and lead-free structure were tackled. Lead-free perovskite solar cells are being researched, but the overall results are not comparable to lead perovskite solar cells [27]. In addition, the perovskite's chemical elements are abundantly available on earth, the cost of chemical resource is low. Because the perovskite solar cells' fabrication process does not require high energy and high cost systems as compared to silicon solar cells, the cost of perovskite solar cells is super competitive [27], [38].

PEROVSKITE SOLAR CELL FABRICATION PROCESS

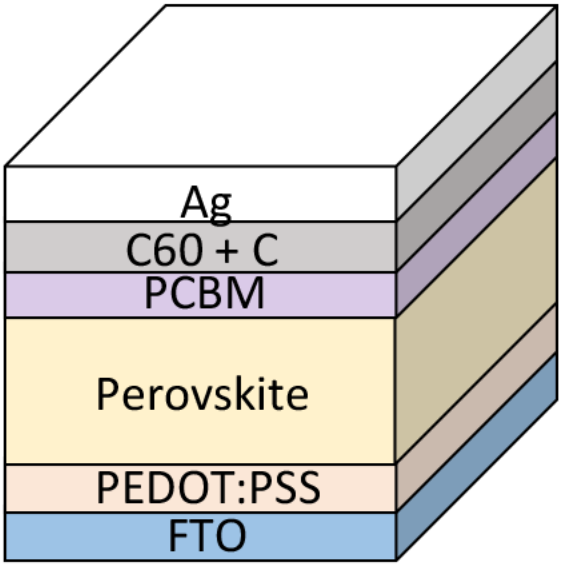

Figure 1. P-i-n inverted structure of perovskite solar cell with PEDOT:PSS as a hole transport layer.

The solar cell fabrication is an intricate process that requires proper handling of chemicals as well as careful transition between the depositions of layers. Figure 1 shows the inverted perovskite solar cell structure that we have been working with. First, we have to prepare a 1 × 1 inch glass, which has a coating of fluorine tin oxide (FTO). Then we defined FTO electrodes for perovskite solar cells. This layer is crucial in the fabrication process as it serves as the conductive layer and the positive contact when taking measurements with the device. The FTO glass is etched in a way to prevent any short connection between the silver layer and the FTO coating. Before we start the fabrication process, it is required to clean the FTO glass to remove any contaminants residing on the surface during the etching and handling process. We prepare three sets of solutions for the cleaning process: methanol, acetone, and 2-propanol. All solution is heated in a hot plate at 80℃ for around 10 minutes, filling the beaker to about 125 mL. We first start with methanol,

place it in the ultrasonic bath for 10 minutes, and repeat the same process for the remaining two chemicals in the order of acetone and 2-propanol being the last chemical used for cleaning. We then dry the glass with a nitrogen gun and bake it for 20 minutes in 120℃ on the hot plate. As we wait for the glass to cool, we then start spin-coating the PEDOT:PSS layer on the glass surface at around 2500 rpm for about 1 minute. Choosing different speeds on the spin coater provides us with different thickness, and choosing 2500 rpm for the PEDOT:PSS provides us with a thickness around ~20 – 30 nm. After spin-coating the PEDOT:PSS layer on the FTO coated glass, we then bake the cell at 150℃ for 15 minutes, and cool it for another 15 minutes. This process allows the crystal structure of the material to return back to its lattice. The next step requires baking the cell for 30 minutes at 180℃ and heating of the perovskite solution at 70℃ in another hot plate. This process requires extensive proper handling as the perovskite layer is responsible for the photo-generation of electrons and holes which are responsible for the current and voltage output of the cell. The temperature of the cell as well as the solution has to be retained during the spin-coating process, thus requiring the handler to properly and quickly transfer the solution onto the glass and start the spin-coating as soon as possible. Not being able to do this properly could output very low efficiencies, shorter lifetime, and a bad J-V curve output. The perovskite structure is spin-coated for about 4000 rpm for 10 seconds to have the thickness of 250 nm. After the spin-coating of the perovskite, we transfered the cell into the glove box and spin-coat the PCBM layer in the glove-box. We spin coat the PCBM layer at 1250 rpm for 1 minute giving us a thickness between 30 – 40 nm. The next step was to deposit a thin layer of C60 mixed with carbon in a ratio of 1:1 using E-beam machine. This deposition had a duration of 20 seconds. Lastly, we then deposit the silver layer at around 120 nm of thickness using the E-beam deposition machine.

Each layer spin-coated and deposited is responsible for certain aspects of how the PSC functions. The silver and FTO glass layer acts as the negative and positive contact when applying voltage measurements to observe the J-V output and efficiency of the cell after fabrication. Furthermore, the PEDOT:PSS layer acts as a hole transport layer (HTL) as it transports the holes and positive ions generated from the perovskite layer as lights hit it. The counterpart PCBM/C60+C layer is responsible for the electron transport (ETL) and negative ions. These two layers are responsible for transporting the electron-hole pairs generated in the perovskite to the contacts during the J-V curve analysis.

CHAPTER II

NICKEL OXIDE

In p-i-n perovskite solar cell structure, PEDOT:PSS is a hole transport layer. It is a popular choice in solar cell structure because of its good conductivity as well as compatible bandgap to let hole passing through. Accordingly, PEDOT:PSS has been used in polymer solar cells and perovskite solar cells [39]–[46]. Unfortunately, PEDOT:PSS has drawbacks such as hygroscopic characteristics as well as a poor electron blocker in solar cells. As a result, perovskite material gets affected by moisture accumulation in PEDOT:PSS layer, which degrades the perovskite solar cell. It was reported that PEDOT:PSS layer made the degradation of organic solar cells more dramatic when compared between low humidity conditions and high humidity conditions [40], [47], [48]. In addition, poor ability to block electron leads to unnecessary recombination at layer interface, which decreases perovskite solar cell performance [40], [46]. The main reason why PEDOT:PSS shows hygroscopic trait is because of PSS characteristic [49]. By itself, PEDOT does not mix into most types of solution. However, the addition of PSS makes PEDOT easily dissolve in water. In addition, the conductivity of PEDOT is decreased because of PSS enclosure [41], [46], [50]. This reduction in conductivity is because of accumulated moisture, which increases sheet resistance [40]. Furthermore, PEDOT:PSS provided by different vendors is originated from different sources and some vendors introduce different amounts of additives [40]; this led to the discoveries made by Norrman et al. [51] where there were unspecified particles formed in the structure of organic solar cells. It was proposed that excess PSS in compared to PEDOT penetrated other layers in organic solar cells and combined with other elements to create observed particles. These particles were defined as point defects in organic solar cells [40], [51]. There were also reports that PEDOT:PSS led to interface degradation due to PSS's high acidity level [49]. Obviously,

PEDOT:PSS is not an ideal material for a hole transport layer in perovskite solar cells. There was research to replace PEDOT:PSS layer with other inorganic material that could transport hole. There are many considerations that need to be considered in choosing a material that can act as a hole transport layer. The material needs to be transparent, being able to block electron, provides ohmic contact with other layers and has good stability [52]–[55].

One of those inorganic materials is a metal oxide material named NiO_x. It has been reported that metal oxide materials provide good stability and better carrier mobility [56]–[58]. In addition, NiO_x is also transparent as well as can act as a hole transporter [55], [59], [60]. NiO_x was first tested out as a replacement of PEDOT:PSS by Irwin et al. [55] and NiO_x demonstrated good potential in organic solar cells [55], [61]. In addition to the satisfaction of transport material requirement, NiO_x also has a work function of between 5 to 5.6 eV. Therefore, NiO_x was deemed as a prospective hole transport layer for perovskite solar cell structures [61].

Even though NiO_x is an ideal candidate to replace PEDOT:PSS, a few problems have been reported associated with NiO_x as a layer of solar cell. Specifically, there is a concern about the conductivity of metal oxide compared to PEDOT:PSS [46]. In addition, NiO_x layer contains a lot of surface defects, which act as potential trap states in solar cell structure [62]. The problem with defects in NiO_x layer is that there was a report of hydroxyl group being absorbed into these sites [63]. Unfortunately, it was reported that hydroxyl group takes part in the degradation perovskite structure [64]. Furthermore, due to a number of trap sites of NiO_x the light soaking effect is imminent, which directly is related to internal defects [65]. With these conductivity and defect concerns accompanying the NiO_x layer, additional steps are needed to rectify these problems if it is to be used as a hole transport layer for perovskite solar cell.

METHODS OF FABRICATING NICKEL OXIDE THIN FILM

In fabricating thin film layer of NiO_x, there are many techniques such as, thermal decomposition of $Ni(OH)_2$ [66], spray pyrolysis [67], [68], sol-gel spin casting [69]–[71], sputtering [72], and thermal oxidation [73].

For thermal decomposition of $Ni(OH)_2$, this process requires the use of six chemicals: nickel chloride hexahydrate, ethanol, hydrazine monohydrate, potassium hydroxide, and acetone [66]. Among these chemicals, the hydrazine monohydrate is a very dangerous chemical since it is highly poisonous and has acute toxicity through oral, dermal, or inhalation. Hence, in order to work with this chemical, the lab scientists would need a glove box filled with noble gas. In addition, the process would require two hours of mixing the chemical and heating temperature as high as 600°C to obtain nickel oxide nanoparticles [66]. It is a very time consuming, energy demanding, and a highly poisonous approach.

For spray pyrolysis, this process requires the mixing of nickel chloride with deionized water and a spraying system that allows noble gas such as nitrogen to act as a carrier to bring the chemical mist to the surface of preheated substrate[67], [68]. The setup of the spaying system is costly and not readily available in our lab.

For sol-gel spin casting method, this process requires the use of nickel acetate tetrahydrate, 2-methoxyethanol, and mono-ethanolamine [69]. In addition, the mixed solution requires more than one day before it can be spin-coated onto the substrate [69]. Another sol-gel spin-coating method requires the use of nickel nitrate hexahydrate, 2-methoxyethanol, mono-ethanolamine, and acetic acid [70]. This process also requires at least two days before the precursor is ready for spin casting on substrate [70]. A third sol-gel spin casting method requires the use of nickel nitrate

hexahydrate, ethylene glycol, and ethylenediamine [71]. It also requires an annealing time of one hour [71]. Therefore, the available sol-gel spin casting methods require a lengthy waiting time and a lot of chemicals to be able to obtain thin film layer of NiO_x. Furthermore, the quickest spin casting method requires the use of ethylenediamine, which has a mark of acute toxicity through oral, dermal, or inhalation.

For the sputtering method [72], this process requires an expensive instrument in order to deposit a thin layer of NiO_x on substrate. Generally, the cost for a sputtering system is more than ten thousand dollars. It is expensive equipment.

For thermal oxidation [73], this process requires the use of an electron beam evaporator, which is very energy consuming equipment with a lengthy processing time. In addition, an electron beam evaporator generally cost more than fifty thousand dollars.

We have developed a facile method to obtain a thin film of NiO_x from a simple mixture of NiO_x powder and HCl solution. This process only needs less than 5 minutes of chemical mixing time and the precursor can be immediately spin casted on top of substrate. In addition, the equipment needed to obtain thin film NiO_x is a spin coater and a hot plate. Furthermore, we do not have to use acute toxic chemicals such as ehylenediamine [71] or hydrazine monohydrate [66] during synthesis process. It is a quick, simple, and inexpensive approach to deposit a thin film layer of NiO_x in place of PEDOT:PSS. It is found that NiO_x greatly increases open circuit voltage and increases the power conversion efficiency compared to PEDOT:PSS.

NEW SYNTHESIS METHOD FOR NiO_x THIN FILM

NiO_x precursor is prepared by mixing 0.72g of NiO with 2 mL of HCl 36% and then stirs at 90°C with 300 rpm speed for 4 minutes. After mixing, the solution is filtered by a 0.45um filter. Figure 2 shows the NiO_x precursor at each stage of chemical mixture.

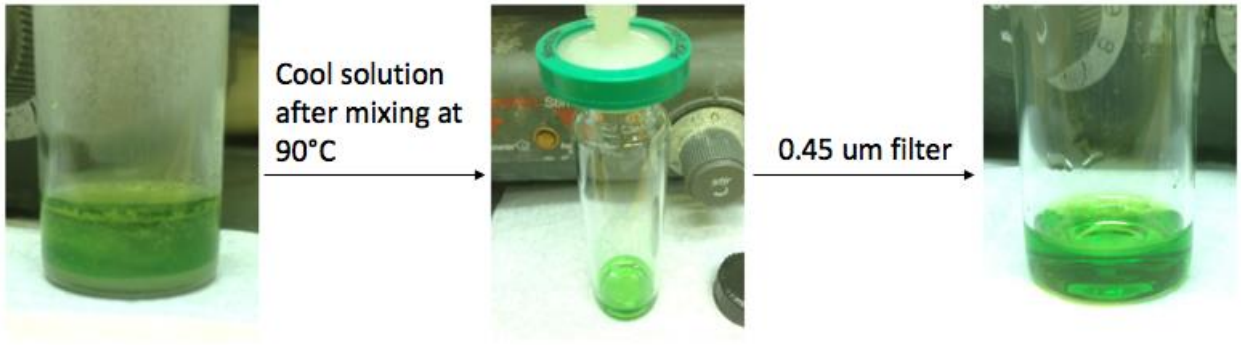

Figure 2. Process of obtaining NiO_x precursor for spin coating method. After mixing NiO_x powder and HCl in 90°C, cooling and filtering were needed to obtain a pristine precursor for spin coating.

The NiO_x precursor is a mixture of nickel chloride ($NiCl_2$) and water (H_2O) as can be seen in the chemical reaction between NiO_x and HCl in equation (1).

$$NiO + 2HCl \xrightarrow{90°C} Ni^{2+} + 2Cl^{-} + H_2O \quad (1)$$

With this simple preparation of NiO_x precursor, the solution is ready to be spin-coated on top of substrate. After spin casting at a speed of 2000 rpm for 60 seconds, the thin layer of solution is then evaporated by heating the glass substrate at 350°C for 10 minutes. The chemical reaction by annealing the solution obtained from equation (1) at 350°C is shown in equation (2).

$$Ni^{2+} + 2Cl^{-} + 6H_2O \xrightarrow{350°C} NiO + 2HCl \uparrow + 5H_2O \uparrow \quad (2)$$

TESTING FOR NICKEL OXIDE STRUCTURE

As this is a new method of depositing NiO_x as a hole transport layer for perovskite solar cell application, we wanted to make sure that we actually obtained a layer of NiO_x. A large amount of solution was deposited onto glass substrate and then evaporated to get a thick layer of material for testing.

X-ray diffraction measurement was done on this substrate afterward. The result is shown in Figure 3. In compared to the x-ray diffraction measurement of a glass surface, the thick surface

of NiO_x showed several NiO_x x-ray diffraction peaks' signature. The x-ray diffraction peaks indicated there were both polycrystalline structure (NiO_x) and crystal structure (NiO) on top of glass substrate. For polycrystalline structure, we clearly observed the x-ray diffraction peaks indexed as (202), (004), (400), and (022) planes [74]. For the crystal structure, we also observed low peaks intensities of crystal planes (111) and (200) [75] in compared to the polycrystalline x-ray diffraction peaks. There was supposed to be a crystal plane (220) visible. However, since the test substrate had a very thick layer of material, there was a lot of noises as can be observed in Figure 3. The (220) crystal plane peak was overwhelmed by noises. Nevertheless, the x-ray diffraction peaks have successfully indicated that NiO_x polycrystalline and NiO crystal structure is obtained from the precursor that we mixed.

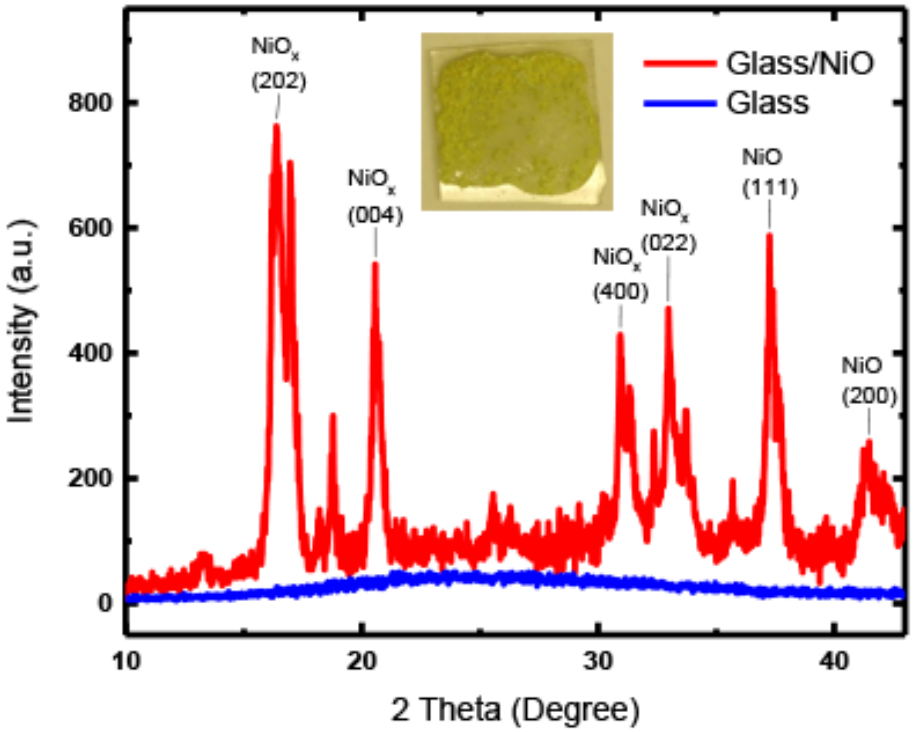

Figure 3. X-Ray diffraction of a thick layer of NiO_x on glass substrate versus glass.

PEROVSKITE'S GRAIN STRUCTURE COMPARISON BETWEEN NiO_x AND PEDOT:PSS

With this new NiO_x deposition method, we would like to know if there would be any difference in perovskite grain structure between the sample with NiO_x and PEDOT:PSS. We prepared two samples with the following structures: FTO/NiO_x/$MAPbI_{3-x}Cl_x$ and FTO/PEDOT:PSS/$MAPbI_{3-x}Cl_x$. Scanning electron microscopy (SEM) measurement was done to compare the perovskite's grain structure. As can be seen in Figure 4, the perovskite grain's structure was similar between the two samples. Hence, there was no structural difference in perovskite layer between samples fabricated with PEDOT:PSS and NiO_x.

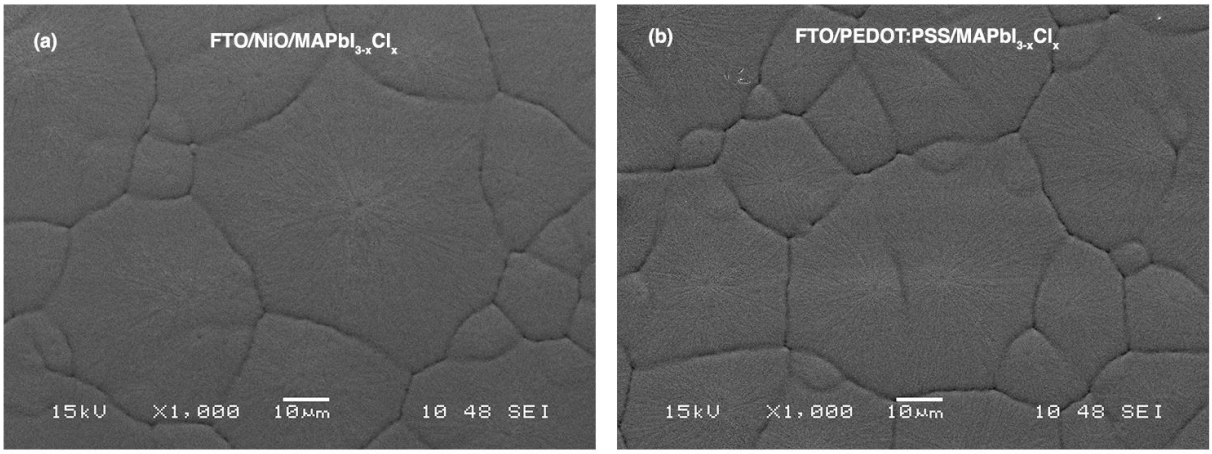

Figure 4. SEM images of (a) FTO/NiO_x/$MAPbI_{3-x}Cl_x$ and (b) FTO/PEDOT:PSS/$MAPbI_{3-x}Cl_x$.

To further investigate the performance difference between the two samples, absorption measurement using ultraviolet–visible spectrophotometry (UV-Vis) instrument was done. The result of this measurement is shown in Figure 5. Interestingly, the absorption amount of the sample using NiO_x deposited by our new method demonstrated a better absorption than the sample with PEDOT:PSS.

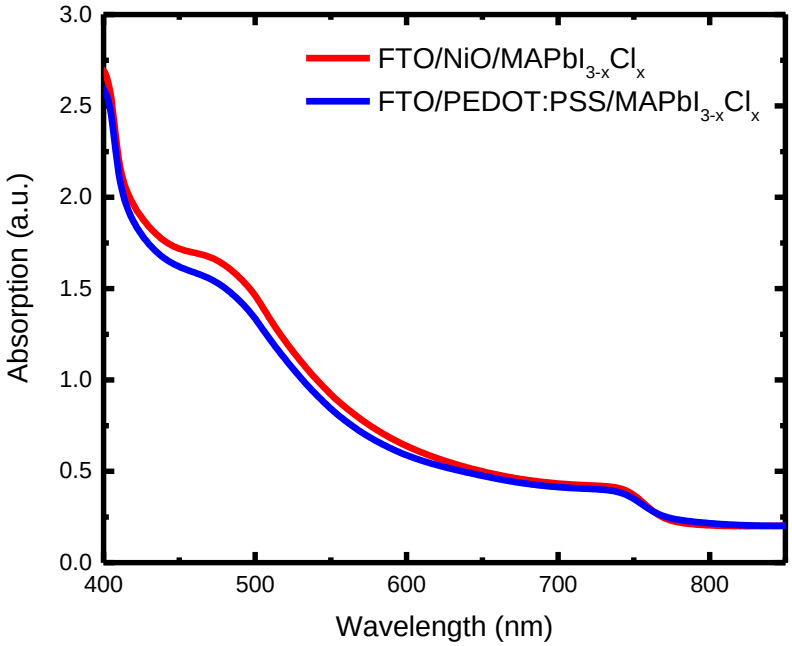

Figure 5. UV-VIS absorption of FTO/NiO_x/$MAPbI_{3-x}Cl_x$ and FTO/PEDOT:PSS/$MAPbI_{3-x}Cl_x$ samples.

An increase in absorption might be a result of higher crystallinity of perovskite since NiO_x is not an organic material and does not contain an acidic component such as PSS that can potentially attack perovskite crystal's structure during and after the sample fabrication process. Hence, the absorption measurement showed that the NiO_x layer obtained by our new deposition method allowed good perovskite crystal grain to absorb light in comparable capacity as the sample with PEDOT:PSS as hole transport layer.

CHAPTER III

PEROVSKITE SOLAR CELL WITH NICKEL OXIDE

Since our method only needs a minimal amount of time to create a mixture of NiO_x powder and HCl solution before spin coating on top of the substrate, we needed to prove that our method created a layer of NiO_x that could replace PEDOT:PSS layer as well as provide better perovskite solar cell structure. To find out whether or not newly developed NiO_x depositing method would result in good perovskite solar cell, two p-i-n perovskite solar cell structures with either NiO_x or PEDOT:PSS as hole transport layer were fabricated.

PEROVSKITE SOLAR CELL FABRICATION WITH NiO_x OR PEDOT:PSS

The perovskite solar cell was fabricated through a series of steps. A glass substrate with FTO coated surface was cleaned using acetone, methanol, and iso-propanol (IPA) sequentially. Each solution was heated at 80°C and then put into an ultrasonic bath for 10 minutes to clean the substrate. The substrate was then dried with nitrogen and heated to 120°C for 20 minutes to completely evaporate all liquid residues. NiO_x precursor was prepared by mixing 0.72g of NiO with 2 mL of HCl 36% and then stir at 90°C with 300 rpm speed for 4 minutes as shown in Figure 2. The solution was then filtered and spin coated onto the substrate at a speed of 2000 rpm for 60 seconds. This substrate was then heated to 350°C for 10 minutes.

PEDOT:PSS precursor was prepared by mixing with IPA for 20 minutes in an ultrasonic bath at a ratio of 1 to 3 before spin coated onto the substrate at a speed of 2500 rpm for 60 seconds. Perovskite ($CH_3NH_3PbI_{3-x}Cl_x$) precursor was prepared by mixing led iodide (PbI_2, Sigma-Aldrich, 99%) and methylamine hydrochloride (MACl, Sigma-Aldrich) at a ratio of 1 to 1 before adding N, N-dimethylformamide (DMF, Sigma-Aldrich, anhydrous, 99.8%) to get an 11% concentration mixture. A hot casting technique was used to create perovskite thin film. The perovskite solution

was heated to 70°C and the substrate was heated to 180°C before spin coating at 4000 rpm for 10 seconds. PCBM(Nano-c) precursor was prepared by mixing with di-chlorobenzene (Sigma-Aldrich). This precursor was spin coated onto substrate in nitrogen filled glove box. C60 mixed carbon and silver contact were the last two layers of perovskite solar cell structure. The mixture of C60 and carbon was in a ratio of 1:1. They were deposited by using electron beam evaporation technique. The completed perovskite solar cell structure were FTO/PEDOT:PSS or NiO_x/$MAPbI_{3-x}Cl_x$/PCBM/C60+C/Ag as shown in Figure 6. The current-voltage measurement was obtained in air by using Keithley 2400 under AM1.5, which emits a power of 100mW/cm^2. In Figure 6(c), the bandgap of NiO_x layer was obtained from [76].

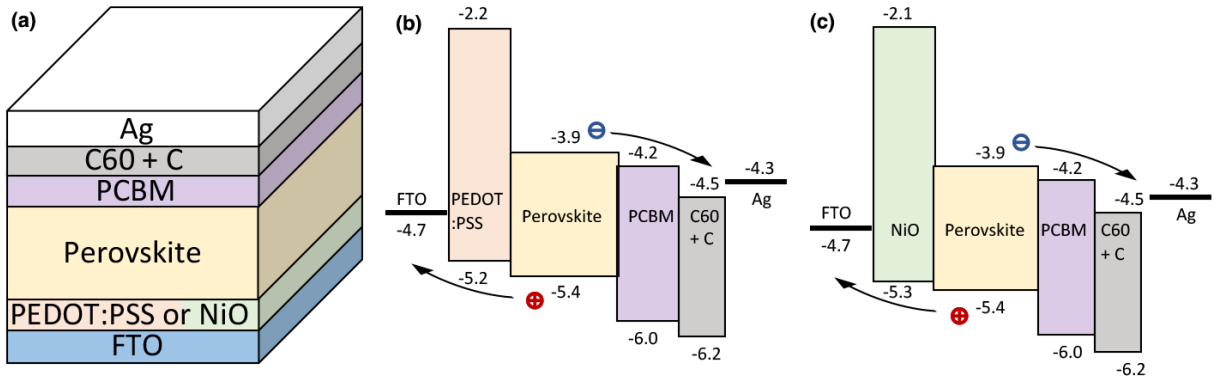

Figure 6. (a) p-i-n inverted structure of Perovskite solar cell with PEDOT:PSS or NiO_x, and energy bandgap alignment of perovskite solar cell with (b) PEDOT:PSS and (c) NiO_x as hole transport layers.

POWER CONVERSION EFFICIENCY

The immediate advantage of replacing PEDOT:PSS layer with NiO_x layer was the increase of open circuit voltage. As can be seen in Figure 7, the perovskite solar cell structure with NiO_x layer had much higher open circuit voltage than the one with PEDOT:PSS layer when both solar cells were made under the same condition.

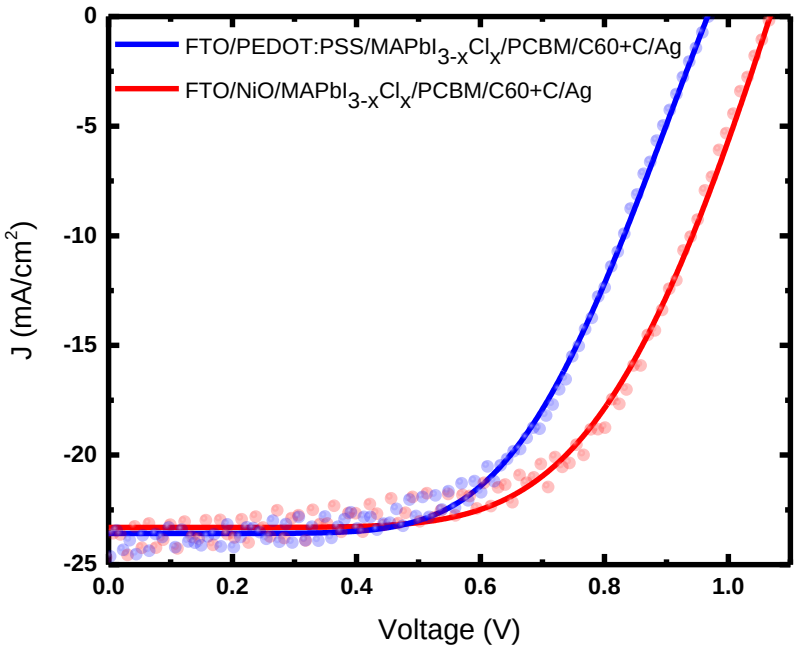

Figure 7. Perovskite solar cell power conversion efficiency comparison between solar cell structure with PEDOT:PSS versus NiO_x. Under the same fabrication condition, the one with NiO_x demonstrated superior performance in comparison to the one with PEDOT:PSS.

Table 1 shows the basic parameters of perovskite solar cell with PEDOT:PSS and NiO_x layer as hole transport layer. The perovskite solar cell structure with PEDOT:PSS as hole transport layer had a power conversion efficiency of 13.04% while the perovskite solar cell structure with NiO_x had a power conversion efficiency of 14.71%. In comparison, the perovskite solar cell with NiO_x had higher open circuit voltage as well as better fill factor. All of these factors contributed to the superior power conversion efficiency of perovskite solar cell with NiO_x versus the one with PEDOT:PSS. According to data obtained from our experiment, open circuit voltage of perovskite solar cell with NiO_x was 10.3% better than the one with PEDOT:PSS. This open circuit voltage

contributed the most to the power conversion efficiency difference between structure with NiO_x and PEDOT:PSS layers.

Table 1. Parameters comparison between solar cell structure with PEDOT:PSS versus NiO_x.

Hole Transport Layer	J_{SC} (mA/cm^2)	V_{OC} (V)	FF	Efficiency (%)
NiO_x	23.30	1.07	0.59	14.71
PEDOT:PSS	23.58	0.97	0.57	13.04

The reason behind higher open circuit voltage for perovskite solar cell is due to the energy bandgap alignment of perovskite solar cell structure. As can be seen in Figure 6(c), the NiO_x layer has a wider bandgap than PEDOT:PSS. In addition, the lowest unoccupied molecular orbital of NiO_x is higher than that of PEDOT:PSS's. This advantage also improves perovskite solar cell ability to prevent electrons from migrating to FTO, which in turn reducing the electron-hole combination effect that would lower the power conversion efficiency of perovskite solar cell.

Positive results were obtained. Under the same condition, the perovskite solar cell with NiO_x yielded improved power conversion efficiency than the one with PEDOT:PSS. Therefore, our simple method of NiO_x deposition had yielded a NiO_x layer that could definitely replace the PEDOT:PSS layer being used as hole transport layer. This initial outcome prompted us to further investigate and optimize the process of depositing NiO_x.

CHAPTER IV

OPTIMIZATION OF PEROVSKITE SOLAR CELL WITH NICKEL OXIDE

As the initial perovskite solar cell with NiO_x as hole transport layer showed good results, we started to optimize fabrication factors such as annealing temperature after spin coating, length of substrate annealing time after spin coating, and the spin speed for optimized thickness of NiO_x layer.

ANNEALING TEMPERATURE OPTIMIZATION OF NICKEL OXIDE LAYER

The first factor that we decided to optimize was the annealing temperature of substrate. We wanted to see if different temperatures of annealing would affect the power conversion efficiency of perovskite solar cell. Four different perovskite solar cells with NiO_x as hole transport layer were made with four different NiO_x layer's annealing temperatures of 300°C, 350°C, 400°C, and 450°C. The J-V curves for these perovskite solar cells are shown in Figure 8. As can be observed, the J-V curves of perovskite solar cell with annealing temperature of 350°C provided the best performance while the one with annealing temperature of 300°C showed no performance.

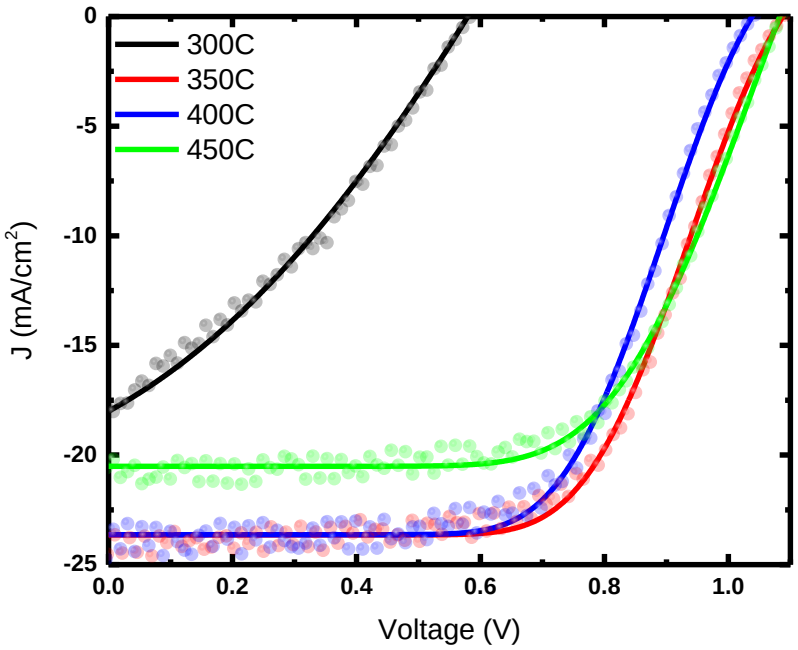

Figure 8. NiO_x based solar cells using annealing temperatures of 300°C, 350°C, 400°C, and 450°C. The solar cell with annealing temperature of 350°C showed the best performance.

Further details of perovskite solar cell parameters are shown in Table 2. Since the perovskite solar cell with annealing temperature of 300°C provided no performance data, it was not included in Table 2. As can be observed, we had the highest efficiency of 16.23% for the perovskite solar cell with annealing temperature of 350°C. The superior short circuit current and open circuit voltage in compared to the parameters from perovskite solar cells with annealing temperatures of 400°C and 450°C were the reasons behind the dominance in power conversion efficiency of perovskite solar cell with annealing temperature of 350°C. Hence, we concluded the best annealing temperature for our perovskite solar cell with NiO_x as hole transport layer is 350°C. The next step is to find out how long we needed to anneal our NiO_x layer to get the best performance.

Table 2. Parameters of NiO_x based solar cells using annealing temperatures of 300°C, 350°C, 400°C, and 450°C.

Temperature (°C)	J_{SC} (mA/cm^2)	V_{OC} (V)	FF	Efficiency (%)
350°C	23.64	1.09	0.63	16.23
400°C	23.63	1.04	0.63	15.48
450°C	20.51	1.08	0.64	14.18

ANNEALING TIME OPTIMIZATION OF NICKEL OXIDE LAYER

With the annealing temperature optimized for NiO_x layer, we wanted to know how long we would need to anneal our NiO_x layer. Hence, we fabricated three different perovskite solar cells with different annealing times of 15 minutes, 30 minutes, and 45 minutes for NiO_x layer. These perovskite solar cells would be annealed at the optimized annealing temperature of 350°C. As can be seen in Figure 9, the annealing time of 15 minutes delivered the best performance of 16.08% power conversion efficiency. The longer annealing time of 30 minutes and 45 minutes lowered the perovskite solar cell performance to 15.62% and 15.55% respectively. Hence, we found that annealing the NiO_x layer at 350°C for 15 minutes delivered the best perovskite solar cells performance so far. These two factors would be used in optimizing the thickness of NiO_x layer through different spin coating speeds.

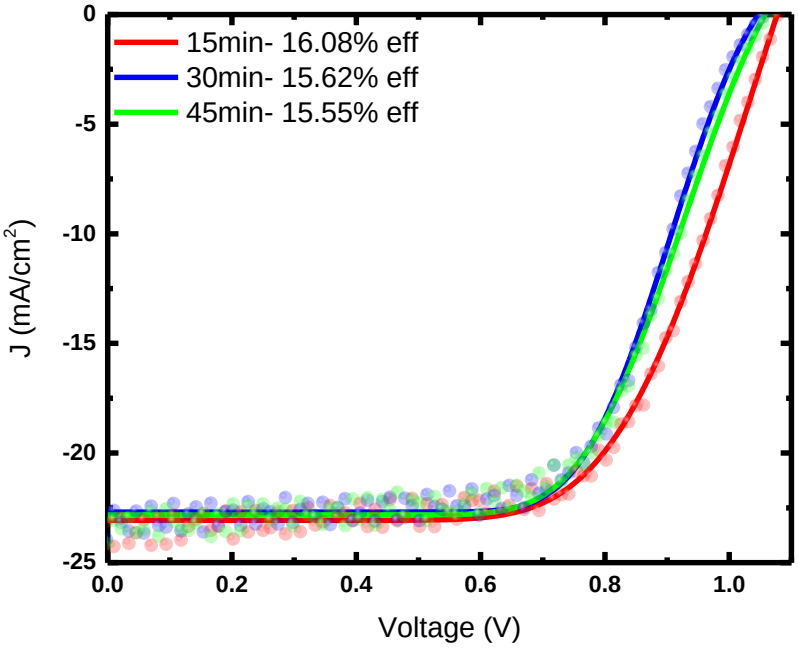

Figure 9. NiO_x based solar cells using different annealing times of 15 minutes, 30 minutes, and 45 minutes at annealing temperature of 350°C.

THICKNESS OPTIMIZATION OF NICKEL OXIDE LAYER

With the annealing temperature and annealing time optimized to be 350°C for 15 minutes, the last optimizing factor that we wanted to do was the thickness of NiO_x layer in perovskite solar cell. Since the thickness of NiO_x layer in our perovskite solar cell structure is directly related to the spin speed after NiO_x precursor deposition, we controlled the different thicknesses of perovskite solar cell with different spin speeds of 1000 rpm, 1500 rpm, 2000 rpm, 2500 rpm, and 3000 rpm. As can be seen in Figure 10, the different thicknesses of NiO_x layer showed significant impact on the performance of perovskite solar cell with NiO_x as hole transport layer. With the spin speed of 3000 rpm, the NiO_x layer was so thin that the performance of perovskite solar cell almost depleted.

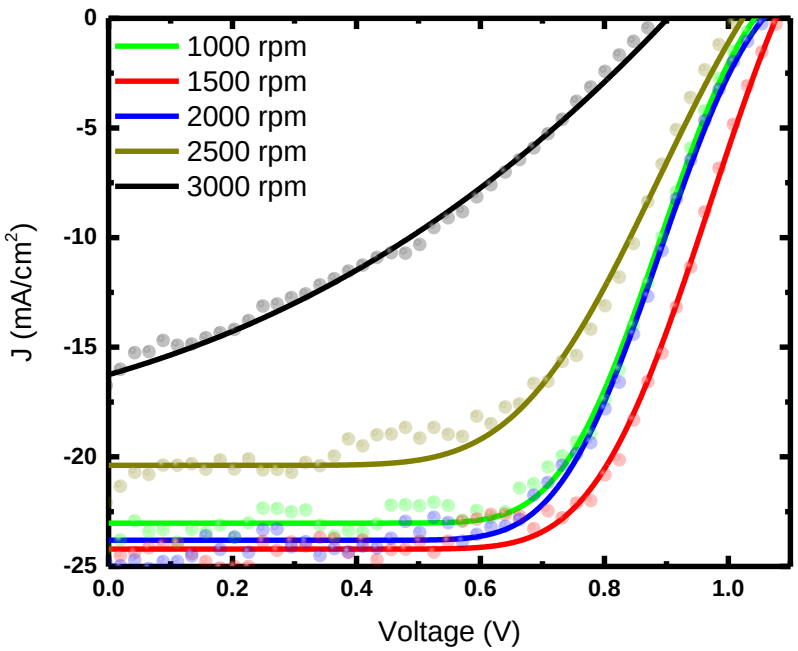

Figure 10. NiO_x based solar cells using different thickness of NiO_x at annealing temperature of 350°C for 15 minutes.

Table 3 shows all the related parameters associated with J-V curves for different thicknesses in Figure 11. The perovskite solar cell with NiO_x layer annealed at 350°C for 15 minutes after spin coating at a speed of 1500 rpm delivered the best power conversion efficiency with 16.76%. For the perovskite solar cell, with spin speed of 1500 rpm, all of the parameters such as short circuit, open circuit voltage, fill factor, and efficiency were superior to the other perovskite solar cells at different spin speed as shown in Table 3. In addition, Figure 11 provides a quick observation on the impact of different thicknesses of NiO_x layer on the perovskite solar cell parameters.

Table 3. Parameters of NiO_x based solar cells using different thickness of NiO_x at annealing temperature of 350°C for 15 minutes.

Thickness (rpm)	J_{SC} (mA/cm^2)	V_{OC} (V)	FF	Efficiency (%)
1000	23.02	1.04	0.63	15.08
1500	24.25	1.08	0.64	16.76
2000	23.80	1.06	0.62	15.64
2500	20.39	1.02	0.57	11.85
3000	16.26	0.90	0.33	4.83

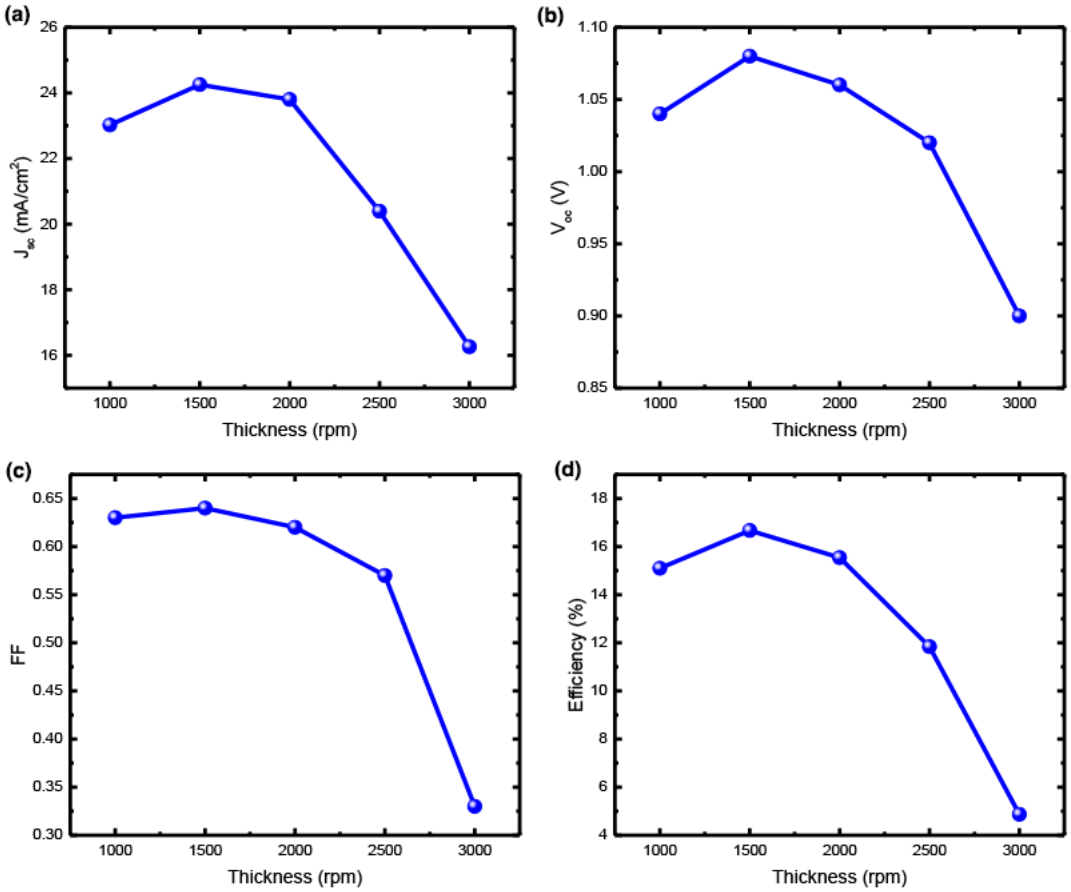

Figure 11. Parameters comparison of NiO_x based solar cells using different thicknesses of NiO_x at annealing temperature of 350°C for 15 minutes.

RESULT AFTER OPTIMIZATION

After optimization of layer thickness, annealing temperature, and annealing time, the power conversion efficiency of perovskite solar cell with NiO_x as hole transport layer had improved from 14.71% in Figure 7 to 16.76% in Figure 12. The parameter difference can be referenced between Table 1 and Table 4. It was the highest perovskite solar power conversion efficiency obtained in our lab so far.

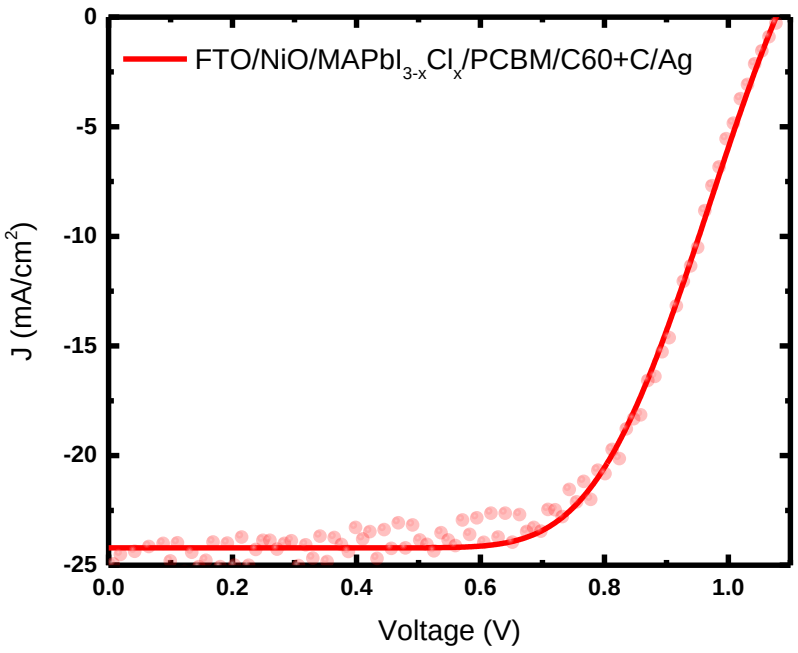

Figure 12. Optimized perovskite solar cell with spin coating speed of 1500 rpm and annealing temperature of 350°C for 15 minutes.

We had optimized fabrication factors such as annealing temperature after spin coating, length of substrate annealing after spin coating, and the spin speed for optimized thickness of NiO_x layer. It was found that the best perovskite solar cell performance was obtained with NiO_x layer spin coating speed of 1500 rpm, annealing temperature of 350°C, and annealing time of 15

minutes. This improvement was the result of better conductivity and higher fill factor as shown in Table 4 in comparison to Table 1.

Table 4. Parameters of optimized perovskite solar cell with spin coating speed of 1500 rpm and annealing temperature of 350°C for 15 minutes.

Hole Transport Layer	J_{SC} (mA/cm^2)	V_{OC} (V)	FF	Efficiency (%)
NiO_x	24.25	1.08	0.64	16.76

CHAPTER V

LIGHT SOAKING EFFECT IN PEROVSKITE SOLAR CELL WITH NICKEL OXIDE

APPEARANCE OF LIGHT SOAKING EFFECT

The perovskite solar cell with NiO_x exhibited light soaking effect. Specifically, the current-voltage measurement of perovskite solar cell increased steadily when it was being exposed with AM1.5 light source. It took more than 10 minutes for the power conversion efficiency to maximize, Figure 13. This phenomenon indicated that there were a lot of defects in this structure of perovskite solar cell, specifically at the NiO_x layer. These defects acted as a trapping location for charge carriers and these points needed to be filled before the solar cell reached its optimum performance potential. These defects might be the result of a low annealing temperature, which result in a high percentage of NiO_x polycrystalline structure versus a low percentage of NiO crystal structure as can be seen in Figure 3.

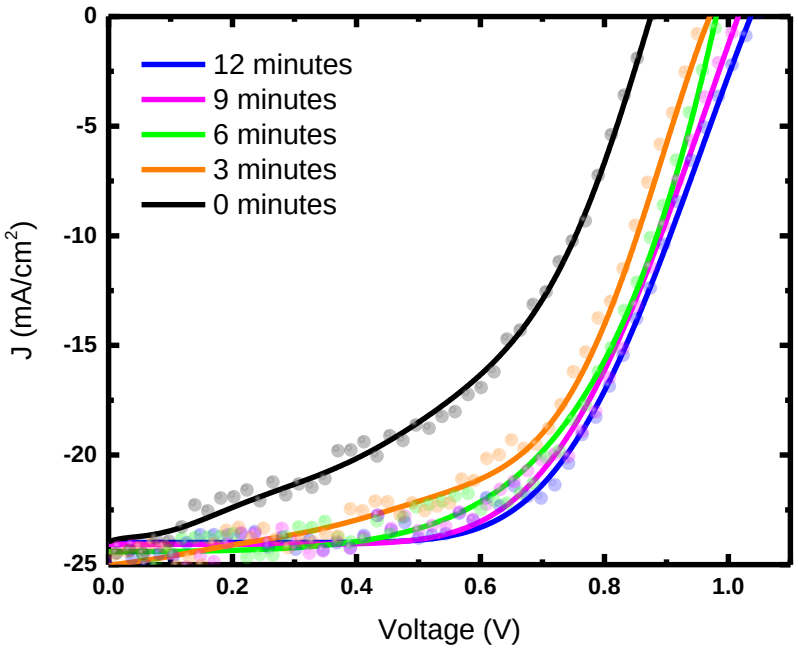

Figure 13. Light soaking effect of Perovskite solar cell with NiO_x as hole transport layer. The J-V curve starts to stabilize after 10 minutes of photo illumination.

REMOVAL OF LIGHT SOAKING EFFECT

As a result of the light soaking effect, further optimization of NiO_x layer was carried out to remove this unwanted effect from happening. We thought that the low temperature of the solar cell substrate contributed to a different percentage of defects in NiO_x layer. Since we had done hot casting of perovskite layer with success in creating high crystallinity grains, we wanted to test if the hot casting technique would help improve the crystallinity of NiO_x layer. The better crystallinity of NiO_x layer would reduce the number of defects, which would lessen the light soaking effect. Hence, we prepared five perovskite solar cells with substrates being annealed at room temperature, 50°C, 70°C, 100°C, and 120°C, before spin coating of NiO_x precursor.

After making perovskite solar cells with different hot casting temperatures as mentioned above, the J-V measurement was done to evaluate the performance difference between each of the perovskite solar cells. By repeatedly doing J-V measurement for each perovskite solar cell while they were being illuminated with AM1.5 light source, we found that the perovskite solar cell with NiO_x layer hot casted at 120°C showed a stable J-V curve before photo illumination and after photo illumination as can be seen in Figure 14.

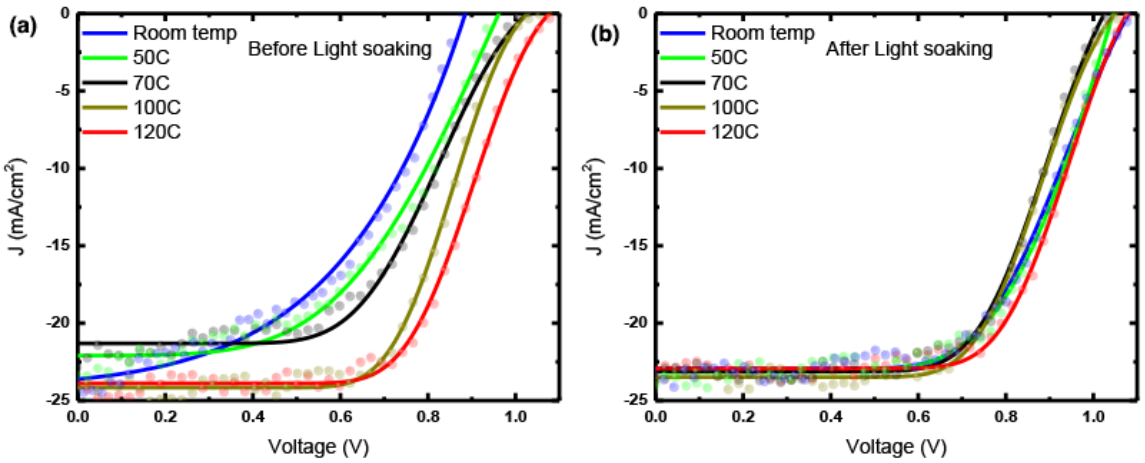

Figure 14. J-V curve of hot casting NiO_x thin film (a) before photo illumination and (b) after photo illumination under AM 1.5 light source. The perovskite solar cell with a hot casting temperature of 120°C was not affected by light soaking process.

For a better perspective on the changes of perovskite solar cells' performance, Figure 15 provides a quick observation of efficiency difference during the illumination time of each solar cell. For the perovskite solar cell spin casting at room temperature, the efficiency of solar cell changes continuously, which is in line with our original finding of light soaking effect in Figure 13. The hot casting temperature showed immediate impact on the reduction of light soaking effect since the higher the hot casting temperature it was, the less the efficiency difference during light

irradiation process. With the observation in both Figure 14 and Figure 15, we concluded that the light soaking effect in our perovskite solar cell with NiO_x as hole transport layer could be removed by doing hot casting at a temperature of 120°C.

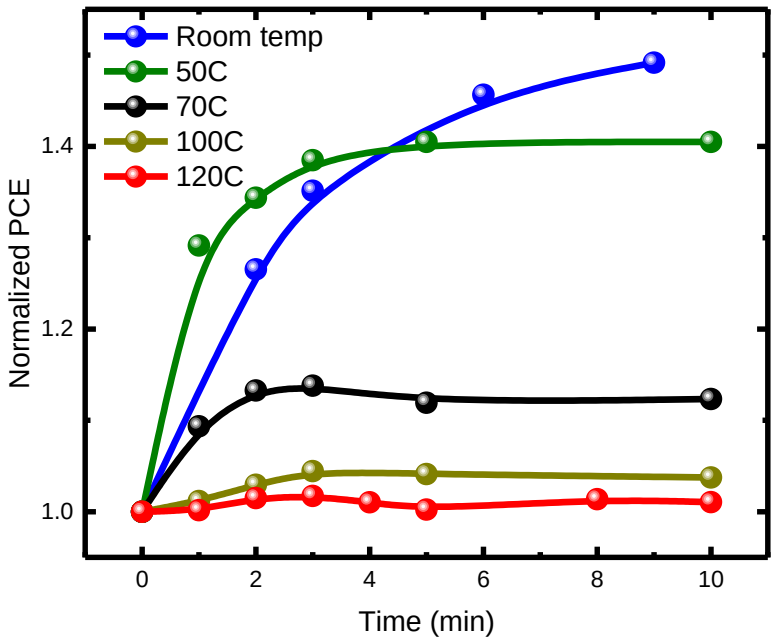

Figure 15. The efficiency difference of all perovskite solar cells with NiO_x thin film hot casted at different temperatures. The one with NiO_x thin film hot casted at 120°C shows stable efficiency during light irradiation.

TIME-RESOLVED PHOTOLUMINESENSE EVALUATION

To understand why perovskite solar cell with hot casting NiO_x thin film layer at 120°C shows almost no signs of light soaking effect, time-resolved PL decays were also measured to evaluate the lifetime of charges between the two perovskite samples structure, FTO/NiO_x room temperature/MAPbI3-xClx and FTO/NiO_x 120°C hot casting/MAPbI3-xClx. We used a time correlated single counting (TCSPC) system to measure time-resolved PL decays with an excitation

source of 450 nm. For our measurement, a power density of 1.15 microwatt at repetition rate of 4 MHz was used. Again, time-resolved PL decays were measured at three different locations for each sample and the average of them was used for analysis. Figure 16 shows the time-resolved PL decays of the two perovskite samples. By observation, the life time decay of perovskite sample with hot casting NiO_x thin film at 120°C had longer decay time than the perovskite sample with spin casting NiO_x thin film at room temperature.

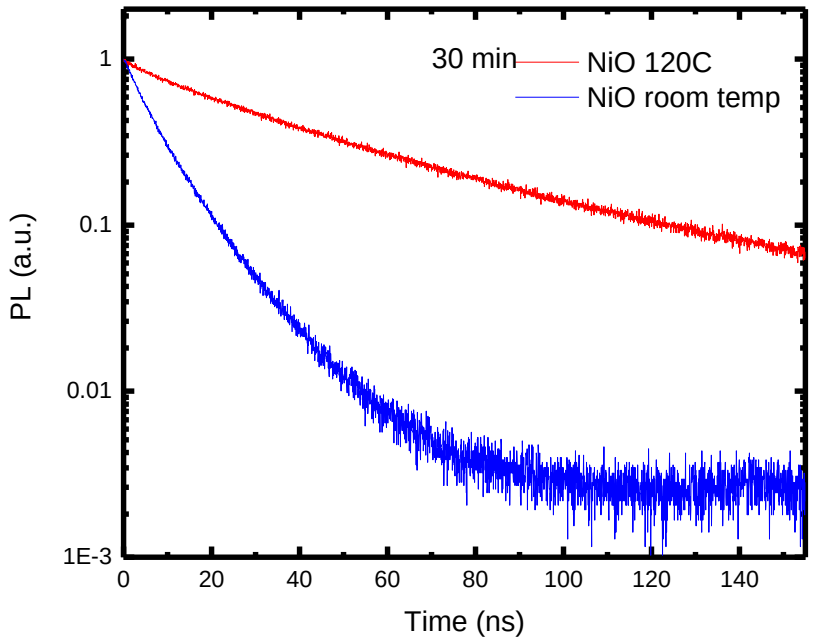

Figure 16. Life decays of FTO/NiO_x room temperature/$MAPbI_{3-x}Cl_x$ and FTO/NiO_x 120°C hot casting/$MAPbI_{3-x}Cl_x$. The perovskite sample with hot casting NiO_x at 120°C showed a significant longer lifetime than the one with NiO_x spin casting at room temperature.

Table 5 shows all parameters of life time decays in Figure 18. These parameters were extracted by fitting those PL decays in Figure 16 with a bi-exponential decay function and lifetime average function:

$$I(t) = A_1 e^{\left(-\frac{t}{\tau_1}\right)} + A_2 e^{\left(-\frac{t}{\tau_2}\right)} \quad (3)$$

$$\tau_{ave} = \frac{A_1\tau_1 + A_2\tau_2}{100} \quad (4)$$

where τ_1, τ_2 and τ_{ave} are fast, slow, and average decay lifetimes and A_1 and A_2 are corresponding weight fractions. Accordingly, the results shown in Table 5 quantitatively show that the perovskite sample with hot casting NiO_x thin film at 120°C had more than four times the average lifetime in comparison to the perovskite sample with spin casting NiO_x thin film at room temperature. In addition, the fast decay weight fraction A_1 of perovskite sample with hot casting NiO_x thin film at 120°C was almost three time less than the corresponding parameter from perovskite sample with spin casting NiO_x thin film at room temperature. The much higher average lifetime and much lower fast decay weight fraction indicated that the perovskite sample with hot casting NiO_x thin film at 120°C had much less defects in NiO_x layer than the perovskite sample with spin casting NiO_x thin film at room temperature.

Table 5. Parameters of life decays of FTO/NiO_x room temperature/$MAPbI_{3-x}Cl_x$ and FTO/NiO_x 120°C hot casting/$MAPbI_{3-x}Cl_x$ after 30 minutes of light irradiation.

Hole Transport Layer	τ_1 (ns)	A_1	τ_2 (ns)	A_2	τ_{ave} (ns)
NiO_x 120°C hot casting	10.95	17.06	49.39	82.94	42.83
NiO_x room temperature	5.00	48.64	12.34	51.36	8.77

With time-resolved PL decay measurement performed, we concluded that spin coating NiO_x thin film at room temperature led to a lot of defects in this layer. As a result, light soaking effect happened because all of the recombination happened at defect sites. However, we were able to successfully remove this light soaking effect by applying hot casting technique to our new

method of spin coating NiO_x thin film. Herein, we have finalized a new method to deposit a thin film of NiO_x as hole transport layer for our perovskite solar cell. This method is very easy to perform and does not require a lengthy process as well as an expensive instrument setup.

CHAPTER VI

CONCLUSIONS

PRIMARY CONTRIBUTIONS OF THIS STUDY

With our quick, simple, and inexpensive approach to fabricate NiO_x thin film, perovskite solar cells with an inverted p-i-n structure, FTO/PEDOT:PSS, or $NiO_x/MAPbI_{3-x}Cl_x$/PCBM/C60+C/Ag, have been investigated. It is found that perovskite solar cell with NiO_x as hole transport layer demonstrated superior open circuit voltage than perovskite solar cell with PEDOT:PSS, which enabled higher solar cell power conversion efficiency. Our experiment has shown that NiO_x thin film obtained by our spin coating technique exhibited good material characteristics such as long decay lifetime. In our experiment, we also removed the light soaking effect cause by defects in NiO_x layer through hot casting technique. This improvement has allowed NiO_x thin film to become the future hole transport layer in our lab since it is so easy to obtain and NiO_x does not cause problems similar to PEDOT:PSS such as unstable chemical quality from manufactures, hygroscopic nature, and an acidic PSS component. Our method does not require the use of highly toxic chemicals such as ehylenediamine, hydrazine monohydrate, expensive spraying, sputtering, electron beam evaporating system, or complex fabrication technique that requires long hours and a lot of chemical mixing. Hence, we have found a quick, simple, and inexpensive method to deposit NiO_x thin film on top of FTO substrate for inverted p-i-n structure of perovskite solar cell.

SUGGESTIONS FOR FUTURE RESEARCH

CARBON QUANTUM DOTS

With the intent to use NiO_x as the hole transport layer, there must be a way to increase the conductivity of this metal oxide material. Not only do carbon quantum dots potentially provide

better conductivity for NiO_x, but also their nanoscale dimensions make it suitable for the thin film layer of perovskite solar cell. There are two approaches in making carbon quantum dots: bottom up and top down. As the bottom up approach requires less specialized equipment, it is also quicker in carbon quantum dots synthesis process. The bottom up approach is the preferred way to fabricate carbon quantum dots in the lab. Regarding the bottom up approach, there are a few fabrication techniques that yield different sizes of the carbon quantum dots. These carbon quantum dots' sizes are directly related to the color emitted from their solutions when high energy light such as deep blue light or ultra violet light, is shined onto their solutions. In addition, different techniques of fabrication result in hydrophilic carbon quantum dots or hydrophobic carbon quantum dots.

Carbon quantum dots were first discovered through carbon nanotubes synthesis process [77]. The small carbon particles illuminated different colors under different nanotube synthesis conditions. Carbon quantum dots were first identified as fragmentation of carbon nanotube during the synthesis process [78]. The discovery of carbon quantum dots sparked interest in finding carbon quantum dots synthesis procedures. Laser ablation was an early method to produce carbon quantum dots from carbon sources. It was also discovered that the carbon quantum dots produced from a laser ablation process did not emit light as expected. It was found that carbon quantum dots produced fluorescence when their surface was treated with additional chemical process. It was concluded that carbon quantum dots' fluorescence property depended on their size, but also depended on the different chemical surface treatment or surface passivation [78], [79]. Another interesting fact about surface passivation of carbon quantum dots is that this process could make carbon quantum dots hydrophilic [78]. After laser ablation method was reported, another approach using carbon based precursors to make carbon quantum dots was described. Because the making of carbon quantum dots from carbon based precursors energetically favored this bottom up process

and it was much simpler than laser ablation of carbon nanotubes [78]. One example would be the shining of a non-focused laser at precursors and achieving controllable carbon quantum dots' size by varying the laser's power [78], [80].

With hydrophilic carbon quantum dots being easier to fabricate since the required chemical materials are readily available in the lab, hydrophilic carbon quantum dots were the first type to be fabricated in the lab. On the other hand, hydrophobic carbon quantum dots were harder to make since the required materials were not available in the lab and were hard to obtain. Ultimately, both hydrophobic and hydrophilic carbon quantum dots were successfully made in the lab. Figure 17 shows the hydrophilic carbon quantum dots that were made in the lab.

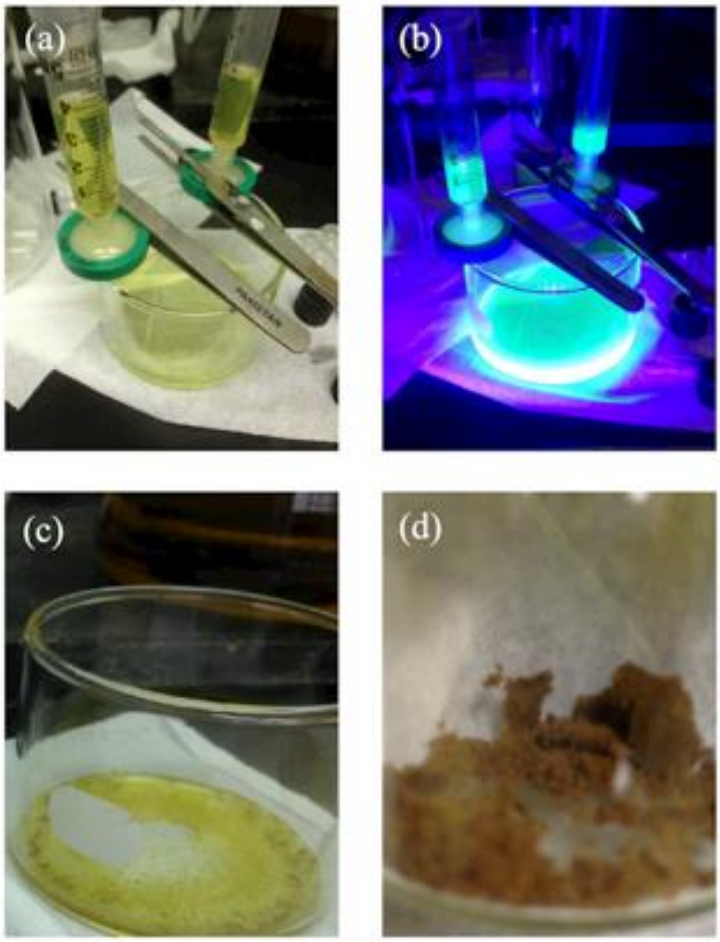

Figure 17. Hydrophilic carbon quantum dots with microwave pyrolysis process is (a) being filtered and (b) shined with blue light. (d) Hydrophilic carbon quantum dots powder (d) is obtained by (c) air drying the solution.

As previously stated, perovskite solar cells degrade easily by moisture. It is ideal to have a hydrophobic electron transport layer to reject moisture from penetrating the perovskite layer. In this instance, carbon quantum dot is a good candidate since there have been reports on synthesizing hydrophobic carbon dots for photovoltaic application. So far, different ways of hydrophobic carbon quantum dots fabrication include: microwave [81], hydrothermal [82], thermal oxidation [83], and material combustion [84]. With the incorporation of hydrophobic carbon quantum dots in perovskite solar cell structure, the air stability of perovskite solar cell has the potential to be

enhanced. Figure 18 shows the successful fabrication of hydrophobic carbon dots solution in the lab.

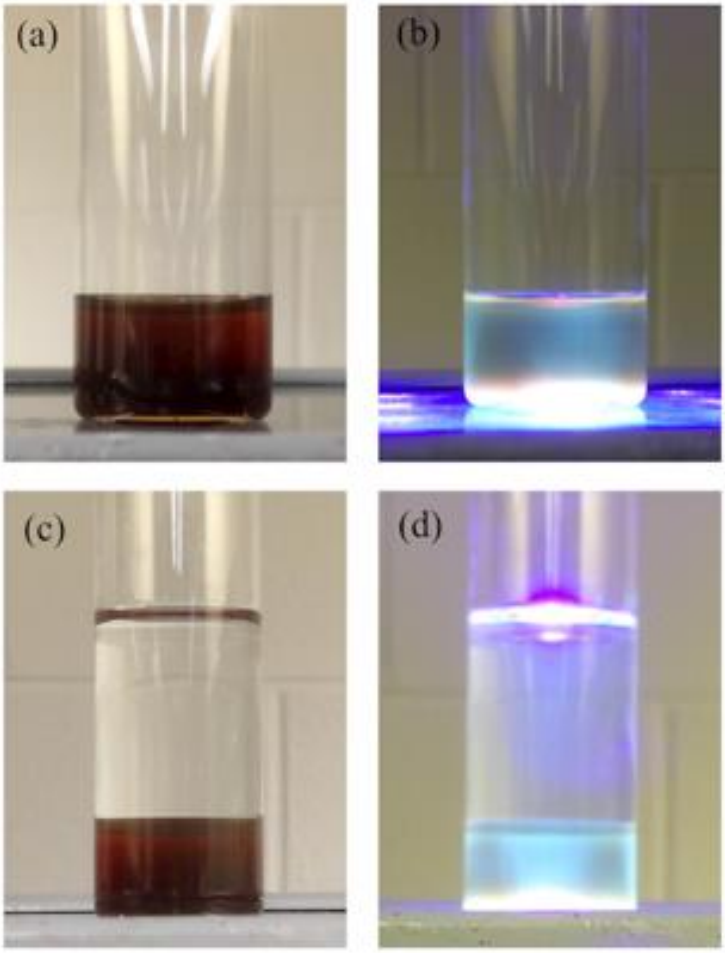

Figure 18. (a) Hydrophobic carbon quantum dots with microwave pyrolysis process, (c) topped with water and (b), (d) shined by blue light.

POLYMETHYL METHACRYLATE

Perovskite solar cells stability is a big issue since perovskite material decomposes with water and air moisture affects the chemical structure of perovskite immensely [27], [85]–[87]. The chemical reaction [27] between perovskite and water is:

$$CH_3NH_3{}^+ + H_2O \rightleftarrows CH_3NH_2 + H_3O^+ \quad (5)$$

$$I^- + H_3O^+ \rightleftarrows HI + H_2O \quad (6)$$

$$CH_3NH_3PbI_3 \rightleftarrows CH_3NH_2 \uparrow + HI \uparrow + PbI_2 \quad (7)$$

Because CH_3NH_2 and HI have -6°C and -34°C boiling points respectively, they turn into gas after perovskite and water reaction. As a result, PbI_2 is the remaining product of perovskite and water reaction. PbI_2 formation can be identified with yellow color and the perovskite crystal can be identified with black color [27]. The degradation of perovskite solar cell after 100 hours can be observed in Figure 19. The changes of all the solar cell parameters are shown in Table 6.

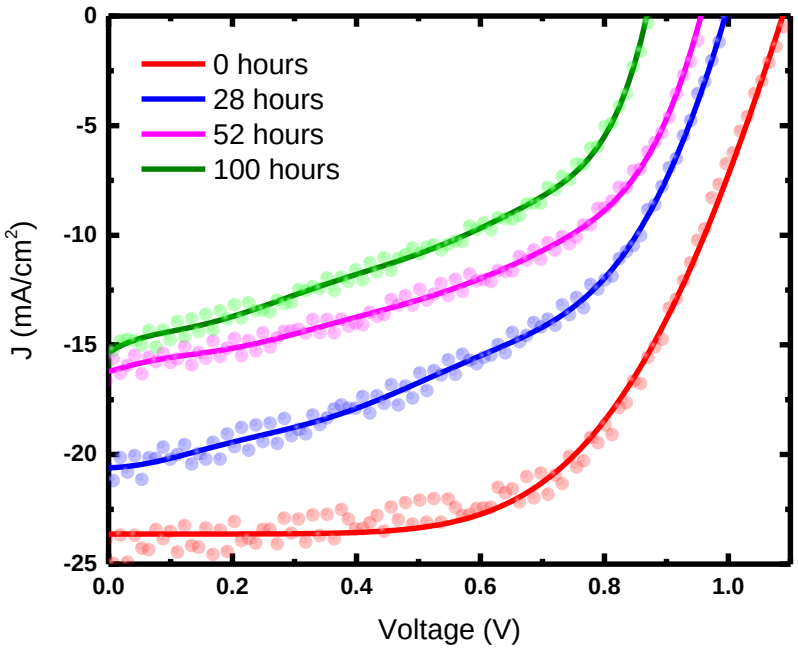

Figure 19. Photo-degradation of Perovskite solar cell with NiO_x as hole transport layer at 0, 28, 52, and 100 hours.

Table 6. Parameter comparison between Perovskite solar cell with NiO_x as hole transport layer at 0, 28, 52, and 100 hours.

Air Exposure Time	J_{SC} (mA/cm^2)	V_{OC} (V)	FF	Efficiency (%)
0 hours	23.63	1.09	0.59	15.20
28 hours	20.61	1.00	0.49	10.10
52 hours	16.22	0.96	0.48	7.47
100 hours	15.36	0.87	0.44	5.88

To increase the air stability of perovskite solar cells, there needs to be a way to prevent moisture from contact with the perovskite layer. Polymethyl methacrylate (PMMA) is a promising material since it has been used to prevent air moisture from penetrating through [88]–[91]. In addition, PMMA was used to passivate perovskite surfaces before [92] and it was also proposed that PMMA structure attached to the dangling terminations of perovskite, which effectively passivates perovskite uneven surfaces [92], [93]. It has been proposed that PMMA can fill into perovskite crystal defect sites, which prevents shorts between electron and hole transporting layer. Perovskite solar cell with PMMA was also reported to withstand air condition for more than 20 days with little degradation [91]. With PMMA being a non-conducting material [93], the mixture of a conductive material such as carbon should lessen the series resistance induced by PMMA. One example was the addition of PCBM to PMMA [93].

REFERENCES

[1] M. C. Scharber *et al.*, "Design Rules for Donors in Bulk-Heterojunction Solar Cells—Towards 10 % Energy-Conversion Efficiency," *Adv. Mater.*, vol. 18, no. 6, pp. 789–794, Mar. 2006.

[2] L.-M. Chen, Z. Hong, G. Li, and Y. Yang, "Recent Progress in Polymer Solar Cells: Manipulation of Polymer:Fullerene Morphology and the Formation of Efficient Inverted Polymer Solar Cells," *Adv. Mater.*, vol. 21, no. 14–15, pp. 1434–1449, Apr. 2009.

[3] W. L. Leong, S. R. Cowan, and A. J. Heeger, "Differential Resistance Analysis of Charge Carrier Losses in Organic Bulk Heterojunction Solar Cells: Observing the Transition from Bimolecular to Trap-Assisted Recombination and Quantifying the Order of Recombination," *Adv. Energy Mater.*, vol. 1, no. 4, pp. 517–522, Jul. 2011.

[4] J. B. Li, V. Chawla, and B. M. Clemens, "Investigating the role of grain boundaries in CZTS and CZTSSe thin film solar cells with scanning probe microscopy," *Adv. Mater. Deerfield Beach Fla*, vol. 24, no. 6, pp. 720–723, Feb. 2012.

[5] A. Singh, H. Geaney, F. Laffir, and K. M. Ryan, "Colloidal synthesis of wurtzite Cu2ZnSnS4 nanorods and their perpendicular assembly," *J. Am. Chem. Soc.*, vol. 134, no. 6, pp. 2910–2913, Feb. 2012.

[6] E. H. Sargent, "Colloidal quantum dot solar cells," *Nat. Photonics*, vol. 6, no. 3, pp. 133–135, Mar. 2012.

[7] B. E. Hardin, H. J. Snaith, and M. D. McGehee, "The renaissance of dye-sensitized solar cells," *Nat. Photonics*, vol. 6, no. 3, pp. 162–169, Mar. 2012.

[8] C. Grätzel and S. M. Zakeeruddin, "Recent trends in mesoscopic solar cells based on molecular and nanopigment light harvesters," *Mater. Today*, vol. 16, no. 1, pp. 11–18, Jan. 2013.

[9] X. Li *et al.*, "Efficient Dye-Sensitized Solar Cells with Potential-Tunable Organic Sulfide Mediators and Graphene-Modified Carbon Counter Electrodes," *Adv. Funct. Mater.*, vol. 23, no. 26, pp. 3344–3352, Jul. 2013.

[10] H. W. Han, W. Liu, J. Zhang, and X.-Z. Zhao, "A Hybrid Poly(ethylene oxide)/ Poly(vinylidene fluoride)/TiO2 Nanoparticle Solid-State Redox Electrolyte for Dye-Sensitized Nanocrystalline Solar Cells," *Adv. Funct. Mater.*, vol. 15, no. 12, pp. 1940–1944, Dec. 2005.

[11] B. O'Regan and M. Graetzel, "A low-cost, high-efficiency solar cell based on dye-sensitized colloidal TiO2 films," *Nature*, vol. 353, pp. 737–740, Oct. 1991.

[12] M. Graetzel, R. A. J. Janssen, D. B. Mitzi, and E. H. Sargent, "Materials interface engineering for solution-processed photovoltaics," *Nature*, vol. 488, no. 7411, pp. 304–312, Aug. 2012.

[13] Z. Liu, B. Sun, T. Shi, Z. Tang, and G. Liao, “Enhanced photovoltaic performance and stability of carbon counter electrode based perovskite solar cells encapsulated by PDMS,” *J. Mater. Chem. A*, vol. 4, no. 27, pp. 10700–10709, Jul. 2016.

[14] Y. Ogomi *et al.*, “CH3NH3SnxPb(1-x)I3 Perovskite Solar Cells Covering up to 1060 nm,” *J. Phys. Chem. Lett.*, vol. 5, no. 6, pp. 1004–1011, Mar. 2014.

[15] H.-S. Kim *et al.*, “Lead iodide perovskite sensitized all-solid-state submicron thin film mesoscopic solar cell with efficiency exceeding 9%,” *Sci. Rep.*, vol. 2, p. 591, 2012.

[16] S. Kazim, M. K. Nazeeruddin, M. Grätzel, and S. Ahmad, “Perovskite as light harvester: a game changer in photovoltaics,” *Angew. Chem. Int. Ed Engl.*, vol. 53, no. 11, pp. 2812–2824, Mar. 2014.

[17] H. S. Jung and N.-G. Park, “Perovskite solar cells: from materials to devices,” *Small Weinh. Bergstr. Ger.*, vol. 11, no. 1, pp. 10–25, Jan. 2015.

[18] Q. Dong *et al.*, “Solar cells. Electron-hole diffusion lengths > 175 μm in solution-grown CH3NH3PbI3 single crystals,” *Science*, vol. 347, no. 6225, pp. 967–970, Feb. 2015.

[19] W. A. Laban and L. Etgar, “Depleted hole conductor-free lead halide iodide heterojunction solar cells,” *Energy Environ. Sci.*, vol. 6, no. 11, pp. 3249–3253, Oct. 2013.

[20] G. E. Eperon, S. D. Stranks, C. Menelaou, M. B. Johnston, L. M. Herz, and H. J. Snaith, “Formamidinium lead trihalide: a broadly tunable perovskite for efficient planar heterojunction solar cells,” *Energy Environ. Sci.*, vol. 7, no. 3, pp. 982–988, Feb. 2014.

[21] J. H. Noh, S. H. Im, J. H. Heo, T. N. Mandal, and S. I. Seok, “Chemical management for colorful, efficient, and stable inorganic-organic hybrid nanostructured solar cells,” *Nano Lett.*, vol. 13, no. 4, pp. 1764–1769, Apr. 2013.

[22] E. Mosconi, A. Amat, M. K. Nazeeruddin, M. Grätzel, and F. De Angelis, “First-Principles Modeling of Mixed Halide Organometal Perovskites for Photovoltaic Applications,” *J. Phys. Chem. C*, vol. 117, no. 27, pp. 13902–13913, Jul. 2013.

[23] N. Arora *et al.*, “Perovskite solar cells with CuSCN hole extraction layers yield stabilized efficiencies greater than 20%,” *Science*, p. eaam5655, Sep. 2017.

[24] A. Kojima, K. Teshima, Y. Shirai, and T. Miyasaka, “Organometal Halide Perovskites as Visible-Light Sensitizers for Photovoltaic Cells,” *J. Am. Chem. Soc.*, vol. 131, no. 17, pp. 6050–6051, May 2009.

[25] A. R. Chakhmouradian and P. M. Woodward, “Celebrating 175 years of perovskite research: a tribute to Roger H. Mitchell,” *Phys. Chem. Miner.*, vol. 41, no. 6, pp. 387–391, Jun. 2014.

[26] C.-H. Chiang, Z.-L. Tseng, and C.-G. Wu, “Planar heterojunction perovskite/PC71BM solar cells with enhanced open-circuit voltage via a (2/1)-step spin-coating process,” *J. Mater. Chem. A*, vol. 2, no. 38, pp. 15897–15903, Sep. 2014.

[27] S. Ito, “Research Update: Overview of progress about efficiency and stability on perovskite solar cells,” *APL Mater.*, vol. 4, no. 9, p. 091504, Sep. 2016.

[28] H. L. Wells, “Über die Cäsium- und Kalium-Bleihalogenide,” *Z. Für Anorg. Chem.*, vol. 3, no. 1, pp. 195–210, Jan. 1893.

[29] D. Weber, “CH3NH3PbX3, ein Pb(II)-System mit kubischer Perowskitstruktur / CH3NH3PbX3, a Pb(II)-System with Cubic Perovskite Structure : Zeitschrift für Naturforschung B,” 01-Dec-1978. [Online]. Available: https://www.degruyter.com/view/j/znb.1978.33.issue-12/znb-1978-1214/znb-1978-1214.xml. [Accessed: 04-Aug-2017].

[30] D. B. Mitzi, S. Wang, C. A. Feild, C. A. Chess, and A. M. Guloy, “Conducting Layered Organic-inorganic Halides Containing <110>-Oriented Perovskite Sheets,” *Science*, vol. 267, no. 5203, pp. 1473–1476, Mar. 1995.

[31] H.-S. Kim *et al.*, “Lead Iodide Perovskite Sensitized All-Solid-State Submicron Thin Film Mesoscopic Solar Cell with Efficiency Exceeding 9%,” *Sci. Rep.*, vol. 2, p. srep00591, Aug. 2012.

[32] M. M. Lee, J. Teuscher, T. Miyasaka, T. N. Murakami, and H. J. Snaith, “Efficient Hybrid Solar Cells Based on Meso-Superstructured Organometal Halide Perovskites,” *Science*, vol. 338, no. 6107, pp. 643–647, Nov. 2012.

[33] N. Ahn, D.-Y. Son, I.-H. Jang, S. M. Kang, M. Choi, and N.-G. Park, “Highly Reproducible Perovskite Solar Cells with Average Efficiency of 18.3% and Best Efficiency of 19.7% Fabricated via Lewis Base Adduct of Lead(II) Iodide,” *J. Am. Chem. Soc.*, vol. 137, no. 27, pp. 8696–8699, Jul. 2015.

[34] W. Chen *et al.*, “Efficient and stable large-area perovskite solar cells with inorganic charge extraction layers,” *Science*, vol. 350, no. 6263, pp. 944–948, Nov. 2015.

[35] D. Bi *et al.*, “Efficient luminescent solar cells based on tailored mixed-cation perovskites,” *Sci. Adv.*, vol. 2, no. 1, p. e1501170, Jan. 2016.

[36] W. S. Yang *et al.*, “High-performance photovoltaic perovskite layers fabricated through intramolecular exchange,” *Science*, vol. 348, no. 6240, pp. 1234–1237, Jun. 2015.

[37] N. J. Jeon *et al.*, “Compositional engineering of perovskite materials for high-performance solar cells,” *Nature*, vol. 517, no. 7535, pp. 476–480, Jan. 2015.

[38] M. Jacoby, “The future of low-cost solar cells | May 2, 2016 Issue - Vol. 94 Issue 18 | Chemical & Engineering News.” [Online]. Available:

http://cen.acs.org/articles/94/i18/future-low-cost-solar-cells.html. [Accessed: 04-Aug-2017].

[39] X. Jia *et al.*, "Highly Efficient and Air Stable Inverted Polymer Solar Cells Using LiF-Modified ITO Cathode and MoO3/AgAl Alloy Anode," *ACS Appl. Mater. Interfaces*, vol. 8, no. 6, pp. 3792–3799, Feb. 2016.

[40] M. Jørgensen, K. Norrman, and F. C. Krebs, "Stability/degradation of polymer solar cells," *Sol. Energy Mater. Sol. Cells*, vol. 92, no. 7, pp. 686–714, Jul. 2008.

[41] D. A. Mengistie, M. A. Ibrahem, P.-C. Wang, and C.-W. Chu, "Highly Conductive PEDOT:PSS Treated with Formic Acid for ITO-Free Polymer Solar Cells," *ACS Appl. Mater. Interfaces*, vol. 6, no. 4, pp. 2292–2299, Feb. 2014.

[42] Z. Jiang *et al.*, "Amazing stable open-circuit voltage in perovskite solar cells using AgAl alloy electrode," *Sol. Energy Mater. Sol. Cells*, vol. 146, no. Supplement C, pp. 35–43, Mar. 2016.

[43] G. Adam *et al.*, "Solution processed perovskite solar cells using highly conductive PEDOT:PSS interfacial layer," *Sol. Energy Mater. Sol. Cells*, vol. 157, no. Supplement C, pp. 318–325, Dec. 2016.

[44] J. Wang, X. Xiang, X. Yao, W.-J. Xiao, J. Lin, and W.-S. Li, "Efficient perovskite solar cells using trichlorosilanes as perovskite/PCBM interface modifiers," *Org. Electron.*, vol. 39, no. Supplement C, pp. 1–9, Dec. 2016.

[45] J. You *et al.*, "Low-Temperature Solution-Processed Perovskite Solar Cells with High Efficiency and Flexibility," *ACS Nano*, vol. 8, no. 2, pp. 1674–1680, Feb. 2014.

[46] H. Luo, X. Lin, X. Hou, L. Pan, S. Huang, and X. Chen, "Efficient and Air-Stable Planar Perovskite Solar Cells Formed on Graphene-Oxide-Modified PEDOT:PSS Hole Transport Layer," *Nano-Micro Lett.*, vol. 9, no. 4, p. 39, Oct. 2017.

[47] K. Kawano, R. Pacios, D. Poplavskyy, J. Nelson, D. D. C. Bradley, and J. R. Durrant, "Degradation of organic solar cells due to air exposure," *Sol. Energy Mater. Sol. Cells*, vol. 90, no. 20, pp. 3520–3530, Dec. 2006.

[48] R. Pacios, A. J. Chatten, K. Kawano, J. R. Durrant, D. D. C. Bradley, and J. Nelson, "Effects of Photo-oxidation on the Performance of Poly[2-methoxy-5-(3′,7′-dimethyloctyloxy)-1,4-phenylene vinylene]:[6,6]-Phenyl C61-Butyric Acid Methyl Ester Solar Cells," *Adv. Funct. Mater.*, vol. 16, no. 16, pp. 2117–2126, Oct. 2006.

[49] M. P. de Jong, L. J. van IJzendoorn, and M. J. A. de Voigt, "Stability of the interface between indium-tin-oxide and poly(3,4-ethylenedioxythiophene)/poly(styrenesulfonate) in polymer light-emitting diodes," *Appl. Phys. Lett.*, vol. 77, no. 14, pp. 2255–2257, Sep. 2000.

[50] D. Alemu, H.-Y. Wei, K.-C. Ho, and C.-W. Chu, “Highly conductive PEDOT:PSS electrode by simple film treatment with methanol for ITO-free polymer solar cells,” *Energy Environ. Sci.*, vol. 5, no. 11, pp. 9662–9671, Oct. 2012.

[51] K. Norrman, N. B. Larsen, and F. C. Krebs, “Lifetimes of organic photovoltaics: Combining chemical and physical characterisation techniques to study degradation mechanisms,” *Sol. Energy Mater. Sol. Cells*, vol. 90, no. 17, pp. 2793–2814, Nov. 2006.

[52] M. S. White, D. C. Olson, S. E. Shaheen, N. Kopidakis, and D. S. Ginley, “Inverted bulk-heterojunction organic photovoltaic device using a solution-derived ZnO underlayer,” *Appl. Phys. Lett.*, vol. 89, no. 14, p. 143517, Oct. 2006.

[53] K. Takahashi, S. Suzaka, Y. Sigeyama, T. Yamaguchi, J. Nakamura, and K. Murata, “Efficiency Increase by Insertion of Electrodeposited CuSCN Layer into ITO/Organic Solid Interface in Bulk Hetero-junction Solar Cells Consisting of Polythiophene and Fullerene,” *Chem. Lett.*, vol. 36, no. 6, pp. 762–763, May 2007.

[54] V. Shrotriya, G. Li, Y. Yao, C.-W. Chu, and Y. Yang, “Transition metal oxides as the buffer layer for polymer photovoltaic cells,” *Appl. Phys. Lett.*, vol. 88, no. 7, p. 073508, Feb. 2006.

[55] M. D. Irwin, D. B. Buchholz, A. W. Hains, R. P. H. Chang, and T. J. Marks, “p-Type semiconducting nickel oxide as an efficiency-enhancing anode interfacial layer in polymer bulk-heterojunction solar cells,” *Proc. Natl. Acad. Sci.*, vol. 105, no. 8, pp. 2783–2787, Feb. 2008.

[56] L. Qian, Y. Zheng, J. Xue, and P. Holloway, “Stable and efficient quantum-dot light-emitting diodes based on solution-processed multilayer structures,” *Nat. Photonics*, vol. 5, no. 9, pp. 543–548, 2011.

[57] S. K. Hau, H.-L. Yip, N. S. Baek, J. Zou, K. O’malley, and A. K.-Y. Jen, “Air-stable inverted flexible polymer solar cells using zinc oxide nanoparticles as an electron selective layer,” *Appl. Phys. Lett.*, vol. 92, no. 25, 2008.

[58] J. You *et al.*, “Improved air stability of perovskite solar cells via solution-processed metal oxide transport layers,” *Nat. Nanotechnol.*, vol. 11, no. 1, p. 75, Jan. 2016.

[59] S. Hüfner, “Electronic structure of NiO and related 3d-transition-metal compounds,” *Adv. Phys.*, vol. 43, no. 2, pp. 183–356, Apr. 1994.

[60] A. Fujimori and F. Minami, “Valence-band photoemission and optical absorption in nickel compounds,” *Phys. Rev. B*, vol. 30, no. 2, pp. 957–971, Jul. 1984.

[61] J.-Y. Jeng *et al.*, “Nickel Oxide Electrode Interlayer in CH3NH3PbI3 Perovskite/PCBM Planar-Heterojunction Hybrid Solar Cells,” *Adv. Mater.*, vol. 26, no. 24, pp. 4107–4113, Jun. 2014.

[62] C. J. Flynn, S. M. McCullough, L. Li, C. L. Donley, Y. Kanai, and J. F. Cahoon, "Passivation of Nickel Vacancy Defects in Nickel Oxide Solar Cells by Targeted Atomic Deposition of Boron," *J. Phys. Chem. C*, vol. 120, no. 30, pp. 16568–16576, Aug. 2016.

[63] N. Kitakatsu, V. Maurice, and P. Marcus, "Local decomposition of NiO ultra-thin films formed on Ni(111)," *Surf. Sci.*, vol. 411, no. 1, pp. 215–230, 1998.

[64] L. Zhang and P. H.-L. Sit, "Ab Initio Study of Interaction of Water, Hydroxyl Radicals, and Hydroxide Ions with CH3NH3PbI3 and CH3NH3PbBr3 Surfaces," *J. Phys. Chem. C*, vol. 119, no. 39, pp. 22370–22378, Oct. 2015.

[65] H. R. Byun, D. Y. Park, H. M. Oh, G. Namkoong, and M. S. Jeong, "Light Soaking Phenomena in Organic–Inorganic Mixed Halide Perovskite Single Crystals," *ACS Photonics*, vol. 4, no. 11, pp. 2813–2820, Nov. 2017.

[66] M. El-Kemary, N. Nagy, and I. El-Mehasseb, "Nickel oxide nanoparticles: Synthesis and spectral studies of interactions with glucose," *Mater. Sci. Semicond. Process.*, vol. 16, no. 6, pp. 1747–1752, Dec. 2013.

[67] M. Jlassi, I. Sta, M. Hajji, and H. Ezzaouia, "Synthesis and characterization of nickel oxide thin films deposited on glass substrates using spray pyrolysis," *Appl. Surf. Sci.*, vol. 308, no. Supplement C, pp. 199–205, Jul. 2014.

[68] P. S. Patil and L. D. Kadam, "Preparation and characterization of spray pyrolyzed nickel oxide (NiO) thin films," *Appl. Surf. Sci.*, vol. 199, no. 1, pp. 211–221, Oct. 2002.

[69] M. Jlassi, I. Sta, M. Hajji, and H. Ezzaouia, "Optical and electrical properties of nickel oxide thin films synthesized by sol–gel spin coating," *Mater. Sci. Semicond. Process.*, vol. 21, no. Supplement C, pp. 7–13, May 2014.

[70] J. Jung, D. L. Kim, S. H. Oh, and H. J. Kim, "Stability enhancement of organic solar cells with solution-processed nickel oxide thin films as hole transport layers," *Sol. Energy Mater. Sol. Cells*, vol. 102, no. Supplement C, pp. 103–108, Jul. 2012.

[71] J. You *et al.*, "Improved air stability of perovskite solar cells via solution-processed metal oxide transport layers," *Nat. Nanotechnol.*, vol. 11, no. 1, p. nnano.2015.230, Oct. 2015.

[72] Y. Zhang, "Thermal oxidation fabrication of NiO film for optoelectronic devices," *Appl. Surf. Sci.*, vol. 344, no. Supplement C, pp. 33–37, Jul. 2015.

[73] J. Jiang, X. Wang, Q. Zhang, J. Li, and X. X. Zhang, "Thermal oxidation of Ni films for p-type thin-film transistors," *Phys. Chem. Chem. Phys.*, vol. 15, no. 18, pp. 6875–6878, Apr. 2013.

[74] S. Rakshit, S. Ghosh, S. Chall, S. Sundar Mati, S. P. Moulik, and S. Chandra Bhattacharya, "Controlled synthesis of spin glass nickel oxide nanoparticles and evaluation of their potential antimicrobial activity: A cost effective and eco friendly approach," *RSC Adv.*, vol. 3, no. 42, pp. 19348–19356, 2013.

[75] H. Yan *et al.*, “Solution growth of NiO nanosheets supported on Ni foam as high-performance electrodes for supercapacitors,” *Nanoscale Res. Lett.*, vol. 9, p. 424, Aug. 2014.

[76] K. X. Steirer *et al.*, “Solution deposited NiO thin-films as hole transport layers in organic photovoltaics,” *Org. Electron.*, vol. 11, no. 8, pp. 1414–1418, Aug. 2010.

[77] K. Hola, Y. Zhang, Y. Wang, E. P. Giannelis, R. Zboril, and A. L. Rogach, “Carbon dots—Emerging light emitters for bioimaging, cancer therapy and optoelectronics,” *Nano Today*, Oct. 2014.

[78] R. Jelinek, “Carbon-Dot Synthesis,” in *Carbon Quantum Dots*, Springer, Cham, 2017, pp. 5–27.

[79] Y.-P. Sun *et al.*, “Quantum-Sized Carbon Dots for Bright and Colorful Photoluminescence,” *J. Am. Chem. Soc.*, vol. 128, no. 24, pp. 7756–7757, Jun. 2006.

[80] H. Yu, X. Li, X. Zeng, and Y. Lu, “Preparation of carbon dots by non-focusing pulsed laser irradiation in toluene,” *Chem. Commun.*, vol. 52, no. 4, pp. 819–822, Dec. 2015.

[81] S. Mitra, S. Chandra, T. Kundu, R. Banerjee, P. Pramanik, and A. Goswami, “Rapid microwave synthesis of fluorescent hydrophobic carbon dots,” *RSC Adv.*, vol. 2, no. 32, pp. 12129–12131, Nov. 2012.

[82] Q.-X. Mao, W.-J. Wang, X. Hai, Y. Shu, X.-W. Chen, and J.-H. Wang, “The regulation of hydrophilicity and hydrophobicity of carbon dots via a one-pot approach,” *J. Mater. Chem. B*, vol. 3, no. 29, pp. 6013–6018, Jul. 2015.

[83] V. Gude, “Synthesis of hydrophobic photoluminescent carbon nanodots by using L-tyrosine and citric acid through a thermal oxidation route,” *Beilstein J. Nanotechnol.*, vol. 5, no. 1, pp. 1513–1522, Sep. 2014.

[84] H. Zhang *et al.*, “Monodispersed carbon nanodots spontaneously separated from combustion soot with excitation-independent photoluminescence,” *RSC Adv.*, vol. 6, no. 10, pp. 8456–8460, 2016.

[85] X. Zhao and N.-G. Park, “Stability Issues on Perovskite Solar Cells,” *Photonics*, vol. 2, no. 4, pp. 1139–1151, Nov. 2015.

[86] B. Philippe *et al.*, “Chemical and Electronic Structure Characterization of Lead Halide Perovskites and Stability Behavior under Different Exposures—A Photoelectron Spectroscopy Investigation,” *Chem. Mater.*, vol. 27, no. 5, pp. 1720–1731, Mar. 2015.

[87] T. Leijtens, G. E. Eperon, N. K. Noel, S. N. Habisreutinger, A. Petrozza, and H. J. Snaith, “Stability of Metal Halide Perovskite Solar Cells,” *Adv. Energy Mater.*, vol. 5, no. 20, p. n/a-n/a, Oct. 2015.

[88] Q. Wang, Q. Dong, T. Li, A. Gruverman, and J. Huang, “Thin Insulating Tunneling Contacts for Efficient and Water-Resistant Perovskite Solar Cells,” *Adv. Mater.*, vol. 28, no. 31, pp. 6734–6739, Aug. 2016.

[89] J. Lee, H. T. Chang, H. An, S. Ahn, J. Shim, and J.-M. Kim, “A protective layer approach to solvatochromic sensors,” *Nat. Commun.*, vol. 4, p. 2461, Sep. 2013.

[90] F. Wang *et al.*, “Highly stable perovskite solar cells with an all-carbon hole transport layer,” *Nanoscale*, vol. 8, no. 23, pp. 11882–11888, 2016.

[91] F. Wang *et al.*, “Highly Efficient and Stable Perovskite Solar Cells by Interfacial Engineering Using Solution-Processed Polymer Layer,” *J. Phys. Chem. C*, vol. 121, no. 3, pp. 1562–1568, Jan. 2017.

[92] W. Kong, T. Ding, G. Bi, and H. Wu, “Optical characterizations of the surface states in hybrid lead–halide perovskites,” *Phys. Chem. Chem. Phys.*, vol. 18, no. 18, pp. 12626–12632, 2016.

[93] J. Peng *et al.*, “Interface passivation using ultrathin polymer–fullerene films for high-efficiency perovskite solar cells with negligible hysteresis,” *Energy Environ. Sci.*, vol. 10, no. 8, pp. 1792–1800, 2017.

VITA

Loi Nguyen

Department of Electrical and Computer Engineering

Old Dominion University

231 Kaufman Hall, Norfolk, VA 23529

I received an Associate of Arts degree in General Studies from University of Maryland University College, Adelphi, MD, in 2015, a Bachelor of Science degree in Electrical Engineering and a Bachelor of Science degree in Computer Engineering from Old Dominion University, Norfolk, VA, both in 2017. The tremendous stress of a maximum course load did not deter me from academic success. I was recognized as at commencement as an Outstanding College Scholar from the Old Dominion University Alumni Association with the highest GPA for both programs in the Batten College of Engineering & Technology.

In summer 2017, through the accelerated BS-MS program, I enrolled into the Master of Science in Electrical and Computer Engineering with focus in enhancement of Perovskite solar cell in the Department of Electrical and Computer Engineering, Old Dominion University, Norfolk, VA. Ever since, I have worked on different perovskite solar cell topics such as, impedance spectroscopy measurement, carbon electrodes fabrication, enhancement of perovskite solar cell structure with PCBM, graphite, or graphene, hydrophilic carbon quantum dots fabrication, hydrophobic carbon quantum dots fabrication, and nickel oxide deposition.

It took ten years to reach a dream and I have learned so much along the path for my education. Currently, I am working as an electrical and computer engineer for the Naval Sea System Command (NAVSEA) doing rapid prototype designs for different military applications.